NBSIR 85-3271

Perimeter Safety Net Projection Requirements

C.W.C. Yancey
N.J. Carino
M. Sansalone

U.S. DEPARTMENT OF COMMERCE
National Bureau of Standards
National Engineering Laboratory
Center for Building Technology
Gaithersburg, MD 20899

November 1985

Issued May 1986

U.S. DEPARTMENT OF COMMERCE
NATIONAL BUREAU OF STANDARDS

NBSIR 85-3271

PERIMETER SAFETY NET PROJECTION REQUIREMENTS

C.W.C. Yancey
N.J. Carino
M. Sansalone

U.S. DEPARTMENT OF COMMERCE
National Bureau of Standards
National Engineering Laboratory
Center for Building Technology
Gaithersburg, MD 20899

November 1985

Issued May 1986

U.S. DEPARTMENT OF COMMERCE, Malcolm Baldrige, *Secretary*
NATIONAL BUREAU OF STANDARDS, Ernest Ambler, *Director*

Perimeter Safety Net Projection Requirements

C. W. C. Yancey, N. J. Carino, and M. Sansalone

ABSTRACT

Current construction-site safety net regulations set limitations on the minimum horizontal projection of perimeter nets and the maximum vertical distance between an elevated working surface and the net below. These limitations were arbitrarily established as no actual or simulated fall data existed. The adequacy of these requirements in ensuring construction worker safety has been questioned. Thus, a test program was carried out to determine the adequacy of existing regulations.

Simulated fall tests were conducted using anthropomorphic dummies to represent falling workers. The dummies fell from a 30-foot (9.1 m) high platform and their trajectories were recorded photographically. The photographs were used to reconstruct the dummies' trajectories and to determine the horizontal distance between the face of the platform and the center of gravity of the dummy. Results are presented to show the trajectory of the falling body and the maximum horizontal distance in the final landing position. An analytical model was developed to simulate a falling worker. The model can be used to predict trajectories for a given set of initial conditions including worker height and weight, departure horizontal velocity and fall height. Guidelines are presented for revising existing regulations pertaining to the dimensional requirements for perimeter nets.

Key words: Construction safety; falling bodies, fall trajectory; horizontal distance; safety nets; simulated falls.

TABLE OF CONTENTS

LIST OF TABLES

LIST OF FIGURES

LIST OF FIGURES cont'd

1. INTRODUCTION

1.1 PERIMETER NET APPLICATIONS

During the construction of a variety of structures such as bridges, high rise buildings and towers, safety nets are used as fall arrestors. The nets are usually assembled on the ground and then hung from the completed portion of the structure at a level specified by regulations. A net which projects from one edge of the structure is referred to as a perimeter or outrigged net. In a typical perimeter net installation the two sides of the net that are parallel to the supporting edge of the structure are attached mechanically to wire cables. The cable supporting the far edge of the net is in turn attached to several tubes, pipes, or cables. The near side cable may be attached to the outriggers, and/or directly to the structure. The outriggers are usually oriented in a diagonal position, extending from the far edge of the net to the supporting member (i.e., beam or column) of the structure. Generally, the connection between one end of the outrigger and the supporting member features a swivel device to permit the assembly to pivot, both during installation and upon impact of a falling object. A typical perimeter net installation is shown in figure 1.1.

1.2 CURRENT REQUIREMENTS FOR PERIMETER NETS

Briefly, an effective perimeter safety net installation must: 1) be wide enough to capture and retain the falling body; 2) be strong enough to withstand the stresses created by the impact of the falling body; 3) be flexible enough to arrest the downward motion without causing serious injury; 4) be placed far enough above rigid or sharp surfaces to prevent "bottoming out"; and 5) optimize the allowable fall distance so that the assembly does not have to be moved too many times. Regulatory requirements for perimeter nets must address these attributes. This report is intended to provide a technical basis for Occupational Safety and Health Administration (OSHA) safety standards for minimum permissible width of net.

In light of the above mentioned objectives, it is helpful to review the current safety net regulations as they pertain to the aforementioned dimensional requirements. The technical provisions of existing safety net standards are tabulated in reference [1]. The list of domestic safety net standards includes: 1) OSHA Part 1926.105; 2) ANSI A10.11-79; 3) U. S. Army Corps of Engineers, 07.D; and 4) California/OSHA Standard, Article 24. Two British documents, CP93-72 and BS3913-73 are also cited in reference [1]. Following is a summary of the regulations related to perimeter nets. For a more comprehensive review of safety net standards the reader should consult reference [1].

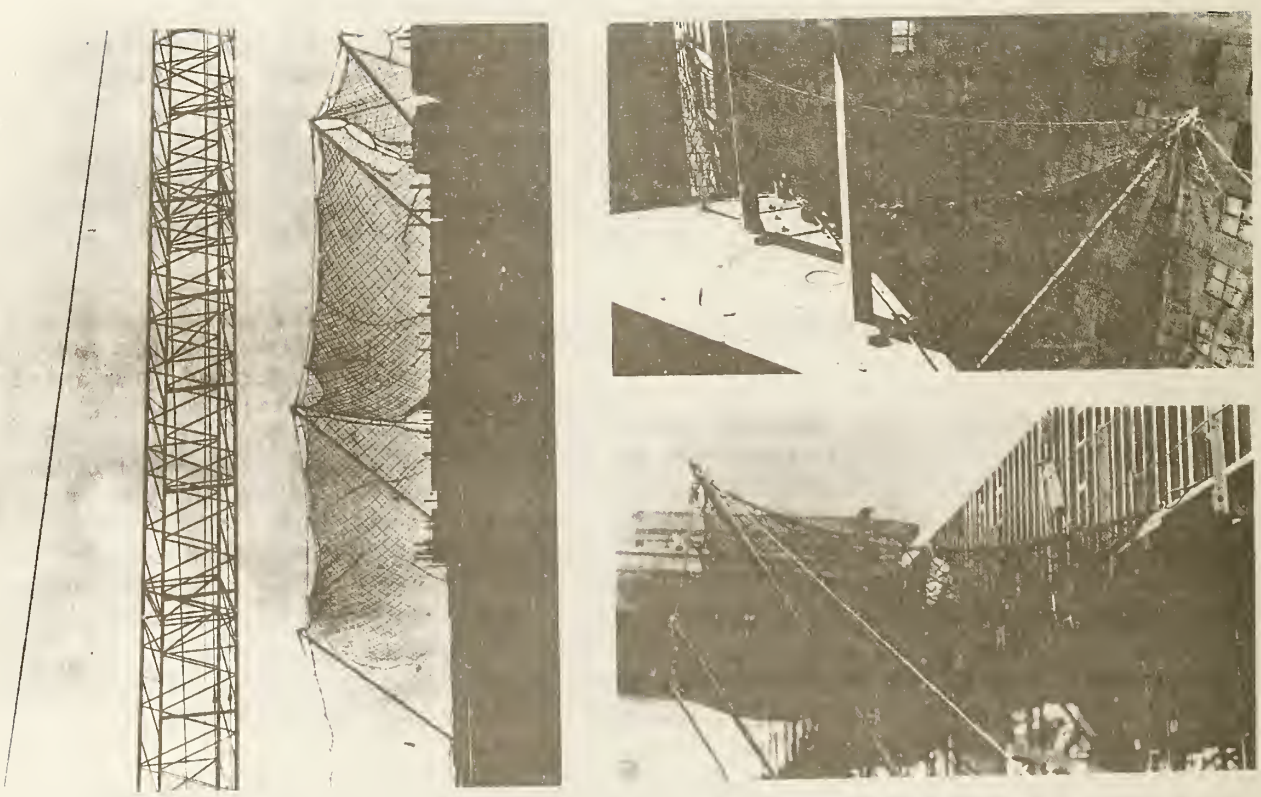

Figure 1.1 Typical perimeter net installation[1]/
1/ Photograph courtesy of Sinco Products Inc.

The minimum horizontal projection of the safety net beyond the edge of the structure is specified as 8 feet (2.4 m) by all four of the U. S. safety net standards. British Code of Practice CP93-72 specifies that outrigged nets should project horizontally a minimum of (2 + H) meters beyond the edge of the working surface, where H is the vertical distance, in meters, between the net and the outermost working point above. The standards differ in their requirements for the maximum allowable distance between the working surface level and the net level. The California/OSHA requirement is the most restrictive; it specifies between working surface level and net level a maximum allowable distance of 10 feet (3.3 m), except in the case of steel erection where the maximum distance is increased to 25 feet (7.7 -m). A 25-foot (7.7-m) limitation is cited in OSHA 1926.105 and in the U. S. Corps of Engineers Standard. British Code of Practice CP93 sets the maximum limit at 6 m (19.8 feet), except in special situations where the maximum distance is increased to 12 m (39.6 feet). The 30 foot (9.1 m) vertical distance permitted by ANSI A10.11-79 is the most liberal regulation. None of the above-mentioned codes are accompanied by a commentary that explains the bases for the limitations that are set on the vertical and horizontal dimensions. This lack of technical basis, coupled with a lack of description of the ways in which construction workers accidentally fall from elevated working surfaces, make it difficult to establish limits for the elevation and projection of perimeter safety nets.

1.3 POSSIBLE FALL CONDITIONS

Typically a construction worker can fall from an elevated working surface by: 1) falling head first from a vertical standstill position, 2) falling head first with some initial horizontal velocity (i.e., walking off the edge), 3) falling head first from a kneeling position, 4) tipping backwards from a crouched position, 5) slipping sideways while walking parallel to the edge of the working surface, 6) being pushed forward or backwards over the edge and 7) walking, tripping or stumbling over an obstruction and being propelled over the edge. These possible fall events are shown schematically in figure 1.2. While there are other possible conditions that could lead to accidental falls, it is felt that those listed above sufficiently define the range of horizontal landing distances that can occur at any given fall height. Because no systematic comparison of the trajectories of construction workers falling from elevated working surfaces have been made, it is not known which sequence of pre-fall events causes the largest horizontal excursion. However, it seems reasonable to assume that, for a given vertical fall height, a sequence including horizontal velocity toward the unguarded edge would lead to a greater horizontal excursion at landing than one with no horizontal velocity toward that edge. Following this line of reasoning, it is deduced that of the events described above,

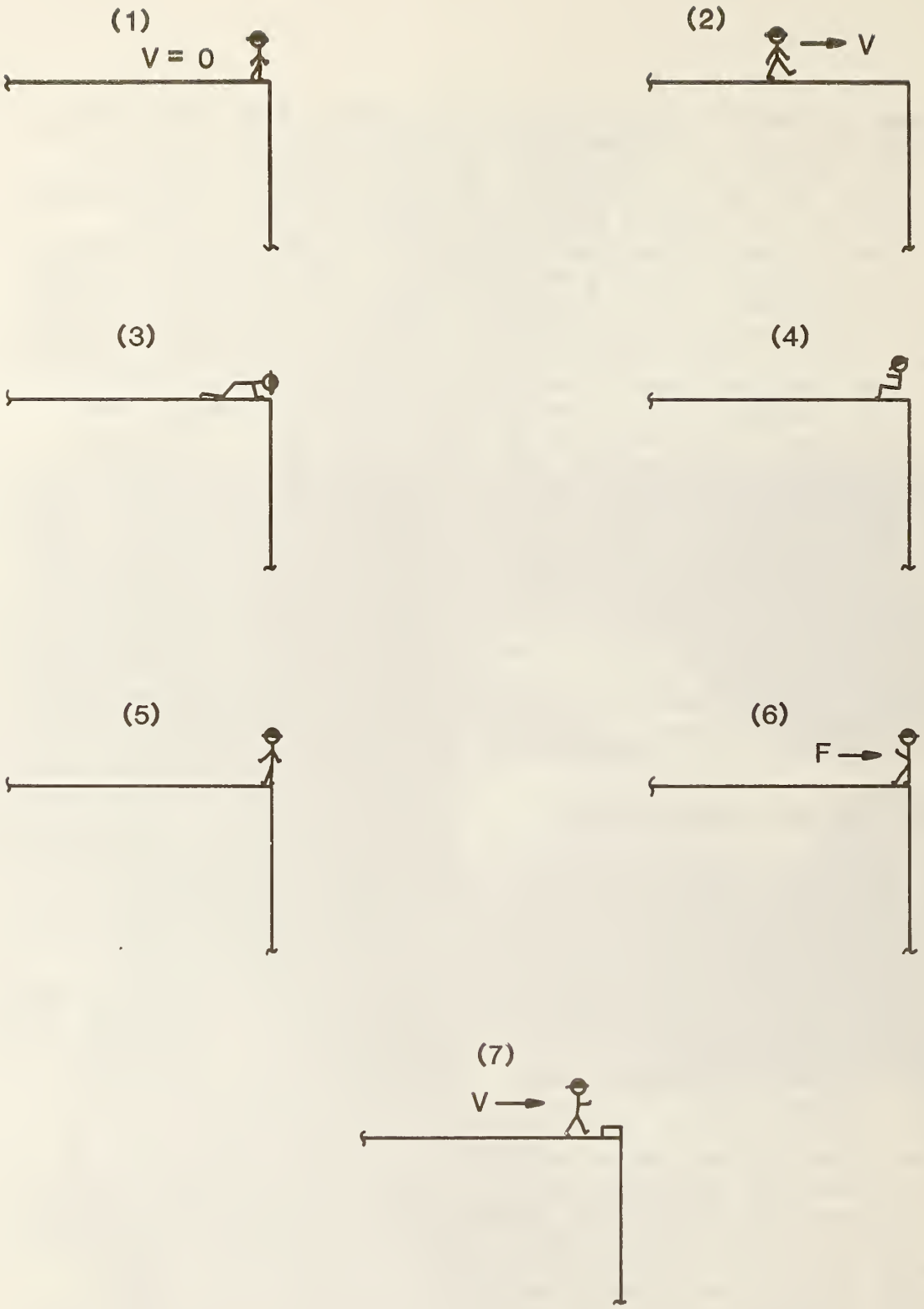

Figure 1.2 Possible conditions leading to accidental falls

number 7 would cause a falling worker to land the greatest distance from the edge.

Two data bases (NTIS and COMPENDEX) were queried in search of data compiled on trajectories and maximum landing distances of falling construction workers. Several reports prepared for the National Institutes for Occupational Safety and Health (NIOSH) and OSHA were identified as possible sources of information. However, a review of these reports revealed that they contain statistical data on such areas as the nature of injuries sustained by various categories of construction worker, age distribution of injured workers, geographic comparisons and seasonal variations in falls. There was practically no data relative to fall trajectories. In addition to performing the above mentioned literature searches, phone contact was made with the National Safety Council, the National Fire Protection Association, NIOSH, OSHA, the Stuntmens Association of California, several local fire departments in major metropolitan areas and two U. S. manufacturers of safety nets. None of these contacts produced any evidence that a systematic comparison of the trajectories of construction workers falling from elevated working surfaces has been made.

A survey of published literature showed that there are no data from ergonomic studies of construction workers on elevated working surfaces from which to ascertain a practical range of walking speeds. The authors conducted a limited study to determine the order of magnitude of "normal" and "fast" walking speeds. Four trial walks were performed by each of three persons, at what was considered to be normal and fast paces. The trials were conducted in an unobstructed corridor that was 363.5 ft (110.8 m) long. A stop watch was used to measure the time required to walk the length of the corridor. The average walking speeds obtained from the trials were: normal, 4.9 fps (1.5 m/s); fast, 6.4 fps (2.0 m/s). In an article in the March 1985 issue of Psychology Today [2], authors R. Levine and E. Wolff report on the results of observations of pedestrians in two American cities. At least 100 people were observed, walking alone, in each city and the times required to walk 100 ft (30.5 m)were measured. The average time required to cover the distance was 22.5 seconds, yielding a rate of 4.4 fps (1.4 m/s). In the simulated fall test study, horizontal velocities of about one-half the normal walking speed determined by Levine and Wolff were used based on the assumption that walking speeds at construction sites on elevated surfaces would be significantly less than normal. In the analytical study, velocities ranging from those used in the fall tests up to those associated with a fast walking pace were used to predict fall trajectories.

1.4 PROBLEM STATEMENT AND TEST OBJECTIVES

1.4.1 Problem Statement

As mentioned above, current U. S. safety net regulations require

a minimum horizontal projection of 8 feet (2.4 m) for perimeter safety net systems. It is reasonable to question the adequacy of the projection requirement for installed perimeter nets for the current limit was established with no technical basis. Moreover, if the current minimum horizontal projection is found to be insufficient the question as to what should be the new minimum limit must be answered.

1.4.2 Test Objective

The first phase of the Safety Nets Standards Study at the National Bureau of Standards was intended to evaluate the existing horizontal projection criteria for perimeter safety nets and to propose new dimensional limits if necessary. Thus, a number of simulated fall tests were conducted using anthropomorphic dummies and a computer model was developed to examine minimum allowable horizontal projection requirements.

2. SIMULATED FALL TESTING

2.1 SELECTION OF THE FALL SEQUENCES TO BE SIMULATED

The objective of the laboratory fall testing was to simulate the trajectories of falling construction workers. It was decided that the testing procedure would focus on creating the effect of a worker who, while walking - either forward or backward - stumbles over an object and falls over an unbarricaded edge of the working surface. Of interest was the descent pattern for a range of fall heights, up to the current maximum of 30 feet(9.1 m). By starting with simulated falls from the 30-ft elevation and filming the sequential positions of the falling body, it was possible to acquire intermediate fall-height data during the course of a single fall test.

2.2 DESCRIPTION OF TEST SETUP AND TEST DUMMIES

2.2.1 Test Setup

The simulated fall tests were performed from a 30-ft (9.1-m)high wooden platform. The elevated platform was attached to a rectangular scaffold made of aluminum tubing. The erected frame measured approximately 40 feet (12.2m) in height and was 8 ft by 4 ft (2.4 m by 1.2 m)in cross section. A 2 ft-6 in (0.8 m) thick padded mat was placed adjacent to the base of the scaffold to provide a landing surface for the falling dummies. The test scaffold and padded mat are shown in figure 2.1. The underside of the 30-ft high wooden platform is shown in the upper left corner of the photograph.

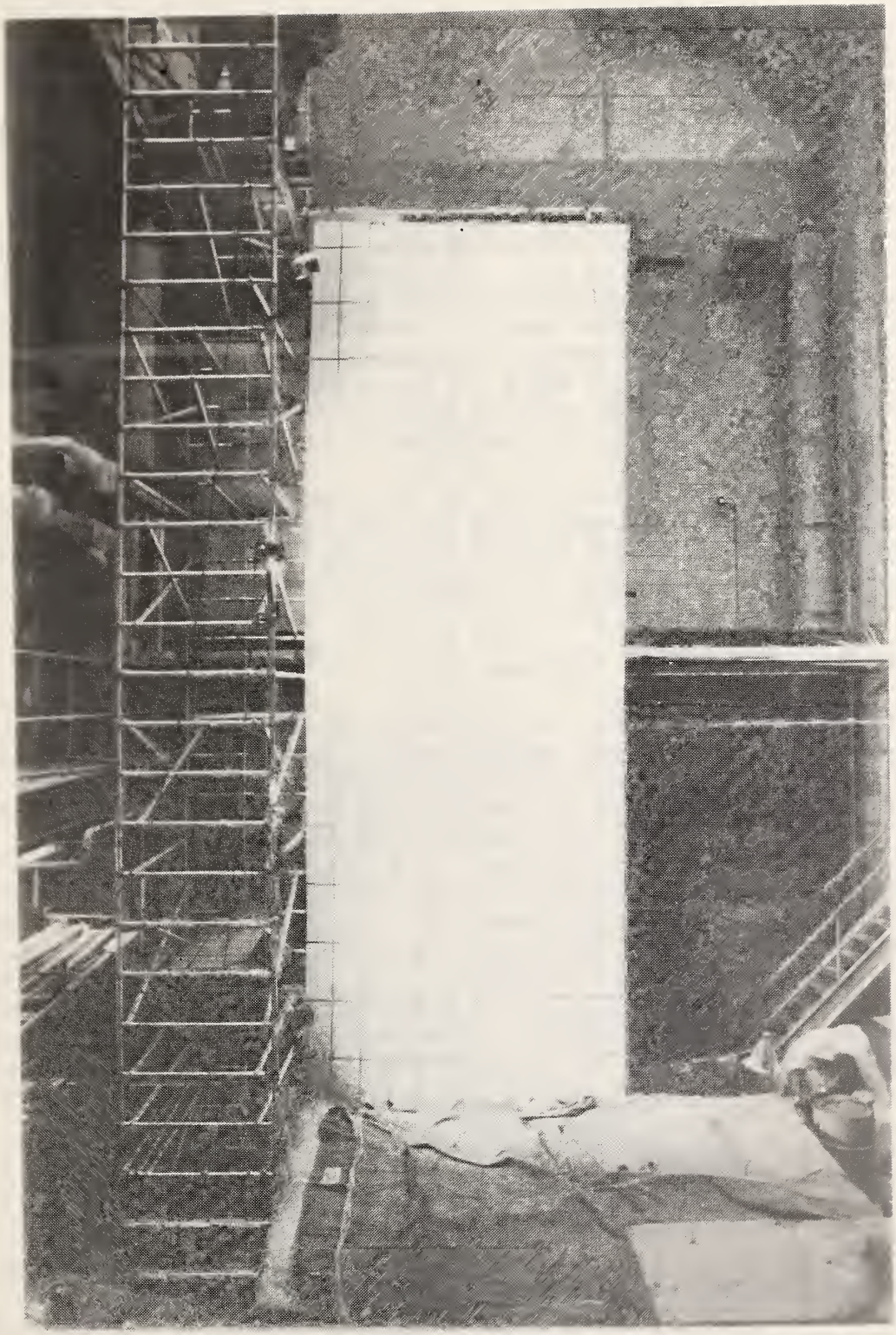

Figure 2.1 Elevation view of test scaffold and padded mat

The dummy was put into motion through the use of an aluminum trolley-track assembly which was installed atop the 30-ft high platform. A side view of the 6-wheeled trolley is shown in figure 2.2. The frame supporting the rails was 5 ft-6 in (1.7 m) long and ran parallel to the 4-ft sides of the wooden platform. Thus, the track extended over the edge of the platform by approximately 18 in (0.5 m). The movement of the trolley was controlled by a pneumatically-actuated cylinder. Attached to the front end of the track frame was a 3/8-in (9.5 mm) aluminum plate which stopped the forward motion of the trolley. The dummy, that was standing near the front edge of the trolley, was thus caused to fall over the unguarded edge of the scaffold in the manner of a worker who stumbles over an obstacle on the working surface.

To aid the photographic recording of the dummies' trajectories, a grid was hung adjacent to one side of the scaffold (see figure 2.1). One vertical edge of the 11 by 30 ft (3.4 by 9.1 m) grid was touching the nearest leg of the scaffold. The grid pattern was 2 ft (0.6 m) vertical by 1 ft (0.3 m) horizontal.

2.2.2 Description of Test Dummies

Two anthropomorphic dummies, with the physical features of 95th and 50th percentile American adult males, were used for making the simulated falls. Their pertinent anthropometric measurements are shown in figure 2.3 and are listed in table 2.1. The 95th percentile dummy used for these tests was in poor mechanical condition compared with the 50th percentile. The 95th percentile dummy had been used in a previous research study on guard rails at the NBS, as well as by the U. S. Department of Transportation for automobile crash tests. As a result of this test history, some of its joints became excessively flexible and had to be retightened after each fall test. On the other hand, the 50th percentile dummy was brand new. Both dummies were used in the erect standing position with the feet squarely planted on the top surface of the trolley and arms down at their sides.

Safety boots were put on the 95th percentile dummy to help stabilize the dummy in the standing position. Furthermore, an upright wooden box was placed at the dummy's back to restrict the tendency to pitch to the side while the trolley was in motion. The box was 5 ft (1.5 m)high and was partially filled with a foam plastic packing material which conformed to the contour of the dummy's back. Thus, prior to each fall test, the dummy was brought in contact with this "mold" and forced into a virtually upright position. The box was permanently attached to the trolley, so that it remained on the trolley as the dummy was propelled over the edge of the scaffold platform.

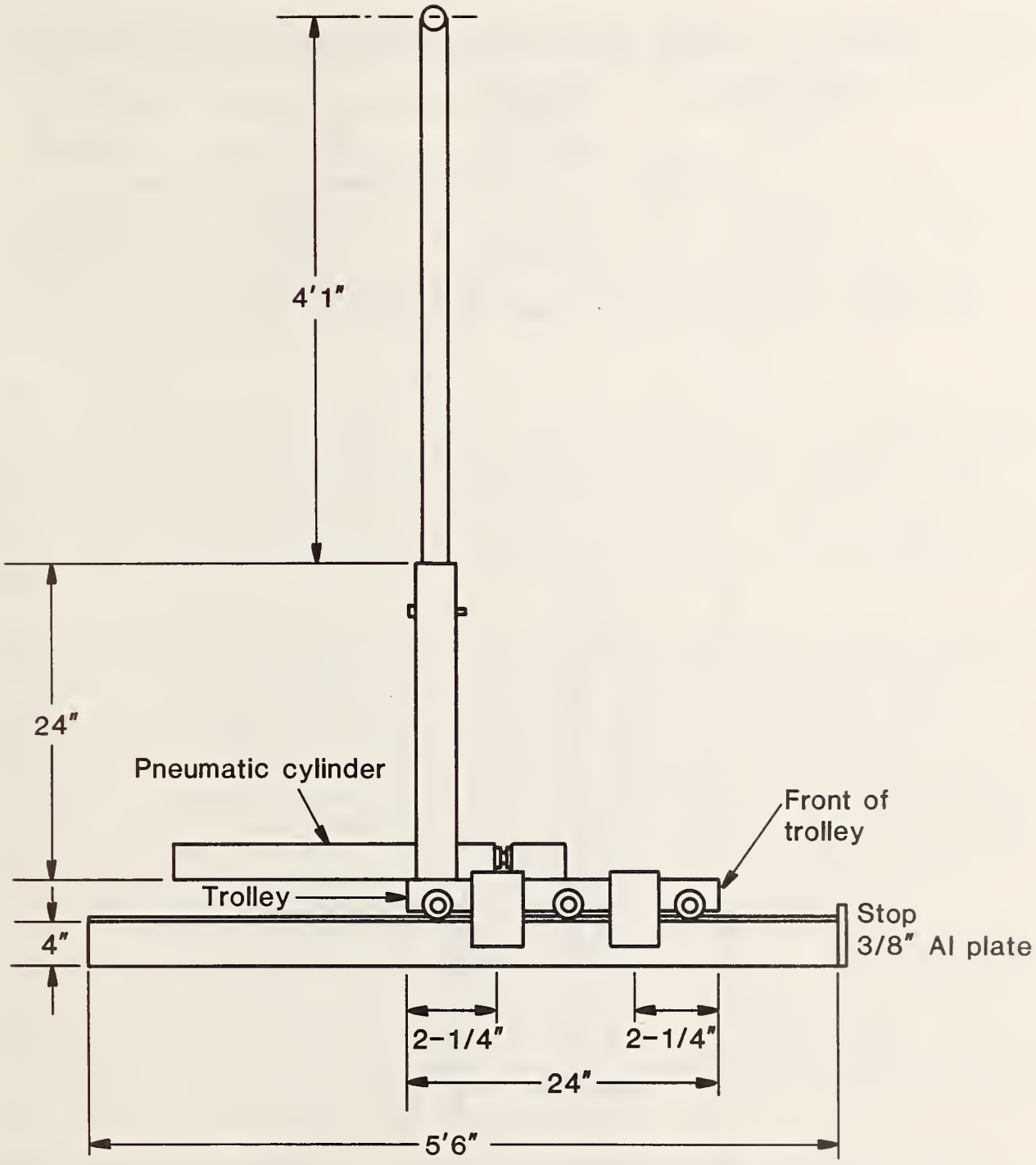

(1 Inch = 25.4 mm)

Figure 2.2 Side view of trolley/track assembly

Table 2.1 Height and weight measurements of test dummies

PERCENTILE	WEIGHT	H	Z[1/]
50th	166 lb	68.3 in	36.9 in
	75.3 kg	1.73 m	0.94 m
95th	217 lb	72.8 in	40.5 in
	98.4 kg	1.85 m	1.03 m

1/ Z was measured while dummy was wearing boots.

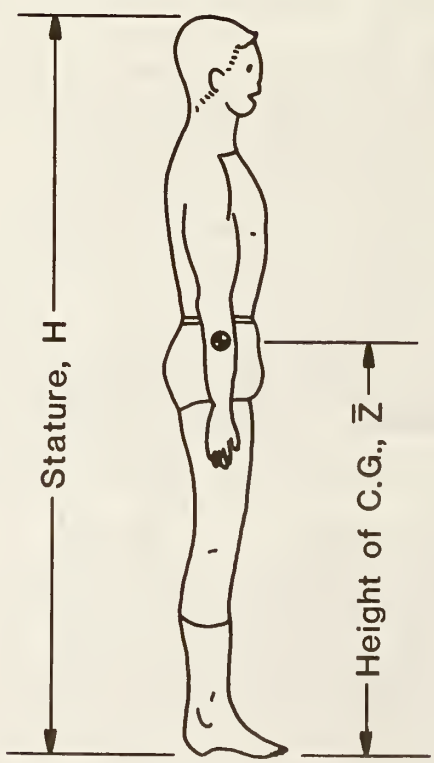

Figure 2.3 Pertinent dimensions of test dummies

Because it had experienced no loss of rigidity in the joints due to previous impacts, the 50th percentile dummy was able to remain in an upright position during the motion of the trolley without the use of boots or a supporting box.

2.3 MEASUREMENT OF TROLLEY HORIZONTAL VELOCITY

To measure the instantaneous horizontal velocity of the loaded trolley immediately prior to impact, the trolley/track/cylinder assembly was set up on the laboratory floor and subjected to a number of trial runs while loaded with dead weights. The dead weights were added in increments of 50 lb (22.7 kg) to effect loads ranging from 50 to 250lb (22.7 to 113.6 kg).

Air pressure for moving the trolley was supplied by the NBS' central compressor, which was the same source of air pressure for the simulated fall tests. Also, the same pressure regulator was used during both the velocity measurement and fall tests. The regulator was preset for various line pressures in increments of 10, ranging from 20 to 80 psi (138 to 552 kPa). For a given load magnitude, there were three trolley runs made for each pressure setting.

The procedure for determining the velocity of the trolley involved the measuring of the time required for two closely-spaced points on the trolley to past a beam of light. The light beam was emitted by a photovoltaic reflective scanner. The scanner was positioned adjacent to the end of the trolley track and its longitudinal axis was directed perpendicular to one side of the track. A light-reflective target was attached to the side of the trolley facing the scanner. The target consisted of a series of black and white strips that were parallel and spaced a known distance apart. Each strip was 1/8 inch (3.1 mm) wide. As the alternate black and white strips of the target passed the scanner, the light beam was reflected to the sensor of the scanner with alternating high and low intensities. The scanner converted these peaks and valleys of light energy into electronic signals which were transmitted to a digital processing oscilloscope. From the known distance between any two strips of the same color (i.e., 0.25 in)and the measured elapsed time between the corresponding peaks or valleys of the recorded waveform, the instantaneous velocity of the trolley was calculated.

There were six samples of time data obtained for each waveform. Thus, for each combination of air pressure and imposed weight there were eighteen velocity values calculated. The average velocity, standard deviation, and coefficient of variation were calculated for each combination. Table 2.2 summarizes the results of the velocity measurements in units of inches per second. Figure 2.4 shows a family of line graphs of velocity versus air pressure for the specified range of dead weights and for the empty trolley.

Table 2.2 Measured trolley speeds for various pressure/weight combinations

PRESS, PSI	AVERAGE SPEED (in/sec) STAND DEVIATION (in/sec.) COEF. OF VARIATION (%) IMPOSED WEIGHT (lb)					
	0	50	100	150	200	250
20	12.2 0.13 1.07	11.2 0.16 1.43	10.82 0.19 1.76	10.10 0.12 1.19	9.53 0.10 1.05	8.85 0.08 0.90
30	19.54 1.43 7.32	18.02 0.13 0.72	16.96 0.12 0.71	16.06 0.17 1.06	15.39 0.13 0.84	14.81 0.12 0.81
40	22.94 0.18 0.78	21.71 0.16 0.74	22.17 0.26 1.17	21.64 0.15 0.69	20.16 0.35 1.74	20.35 0.13 0.64
60	24.03 0.16 0.67	24.31 0.16 0.66	23.63 0.38 1.61	23.61 0.25 1.06	23.39 0.11 0.47	22.81 0.12 0.53
80	24.22 0.10 0.41	24.22 0.29 1.20	24.49 0.30 1.22	24.47 0.31 1.27	23.66 0.19 0.80	23.53 0.33 1.40

1 psi = 6.894 kPa
1 in/sec = 25.4 mm/sec
1 lbm = 0.454 kg

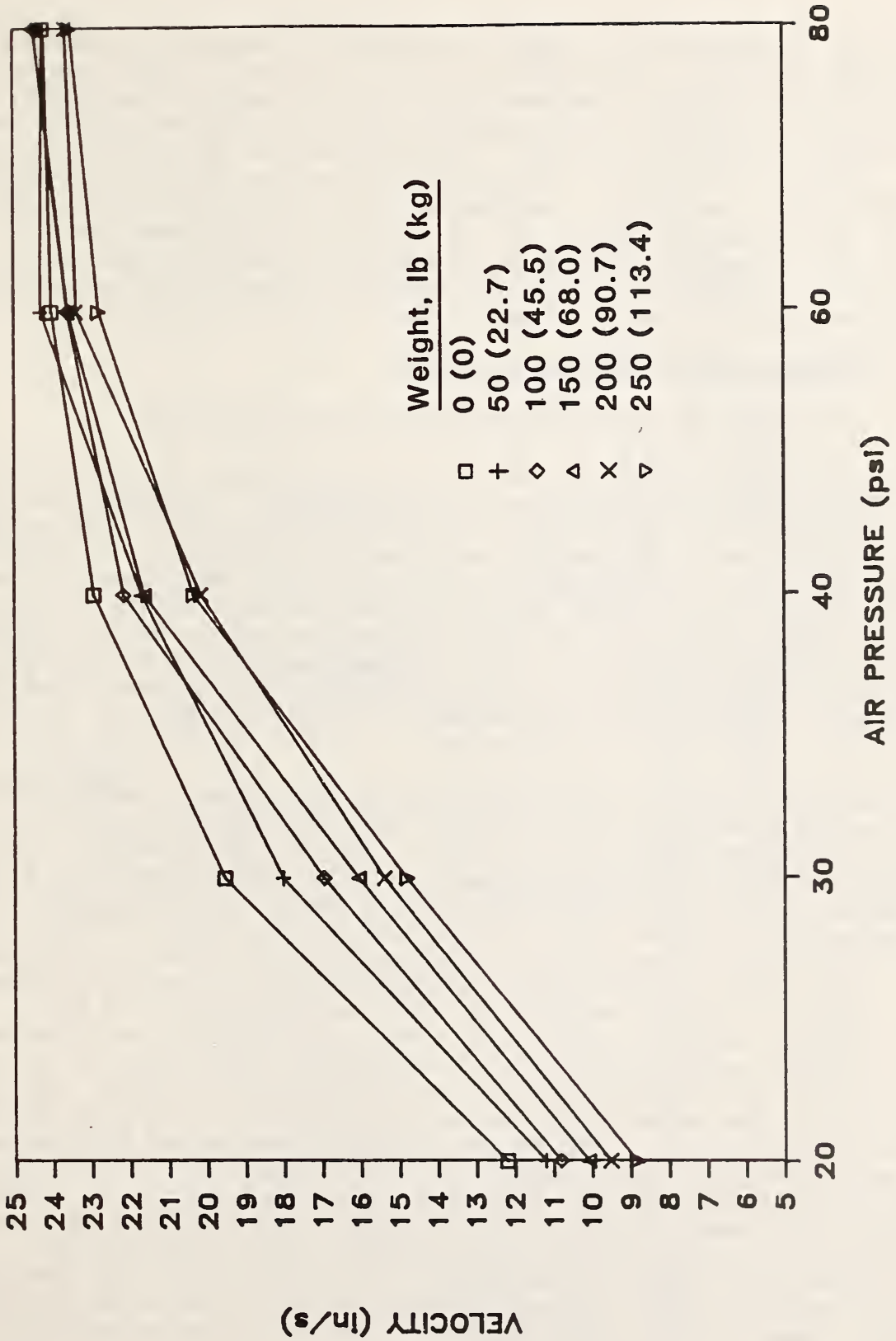

Figure 2.4 Velocity measurements of the trolley

Referring to figure 2.4, there are several noteworthy observations about the velocity measurements of the trolley. There was a nonlinear relationship between the pressure and the velocity of the trolley. Compare, for example, the velocity magnitudes at 40 and 80 psi (276 and 552 kPa). At pressures of 20, 30 and 40 psi (138, 207 and 276 kPa), the lesser the imposed weight the greater the horizontal velocity. Beginning with 60 psi (414 kPa), the effect of increased weight on the velocity magnitudes was diminished. In fact, at 80 psi (552 kPa) there was only a difference of about 1 in/sec (25 mm/sec) between the velocities of the empty and heavily loaded (i.e. 250 lb) trolley.

2.4 PHOTOGRAPHIC RECORDING OF FALLS

2.4.1 Procedure for Observing the Fall Trajectories

One of the principal parts of the test procedure was the photographic recording of the trajectories of the dummies, including the point of impact with the padded mat. The total time of fall from the test platform was computed to be about 1.5 seconds. In order to photographically record four or five discrete positions of the body's center of gravity, both the times of the camera's shutter opening and closing and the film advancing had to be less than 300 milliseconds (1500/5). In fact, because the dummy's body would be accelerating vertically downward, it was concluded that the camera system had to be capable of photographing an event at least once every 200 milliseconds.

The technique used to photographically record fall trajectories involved the use of a 35-mm single lens reflex camera with a motor drive for advancing the film. The motor drive unit was capable of continuous film advance at the maximum rate of 5 frames per second. The motor drive's shutter release button was depressed at the same time as the trolley was set in motion. The filming was continuous until the dummy came to rest on the padded mat. After some preliminary experimentation, it was concluded that a shutter speed setting of 1/250 sec produced the best photographic results. The camera was equipped with a wide-angle lens (28 mm) and ASA 400 film. The camera was placed on a tripod and located on a scaffold platform such that the center of the lens was at the same elevation as the center of the grid pattern shown in figure 2.1. The camera platform was moved sufficiently far away from the test scaffold to allow the entire vertical distance between the test platform and padded mat to be viewed through the camera's lens. In addition, the platform was squared with respect to the plan of the gridded cloth backdrop and positioned such that a line segment from the center of the grid to the center of the lens was perpendicular to both the backdrop and the camera body. An elevation view of the above mentioned setup is shown in figure 2.5.

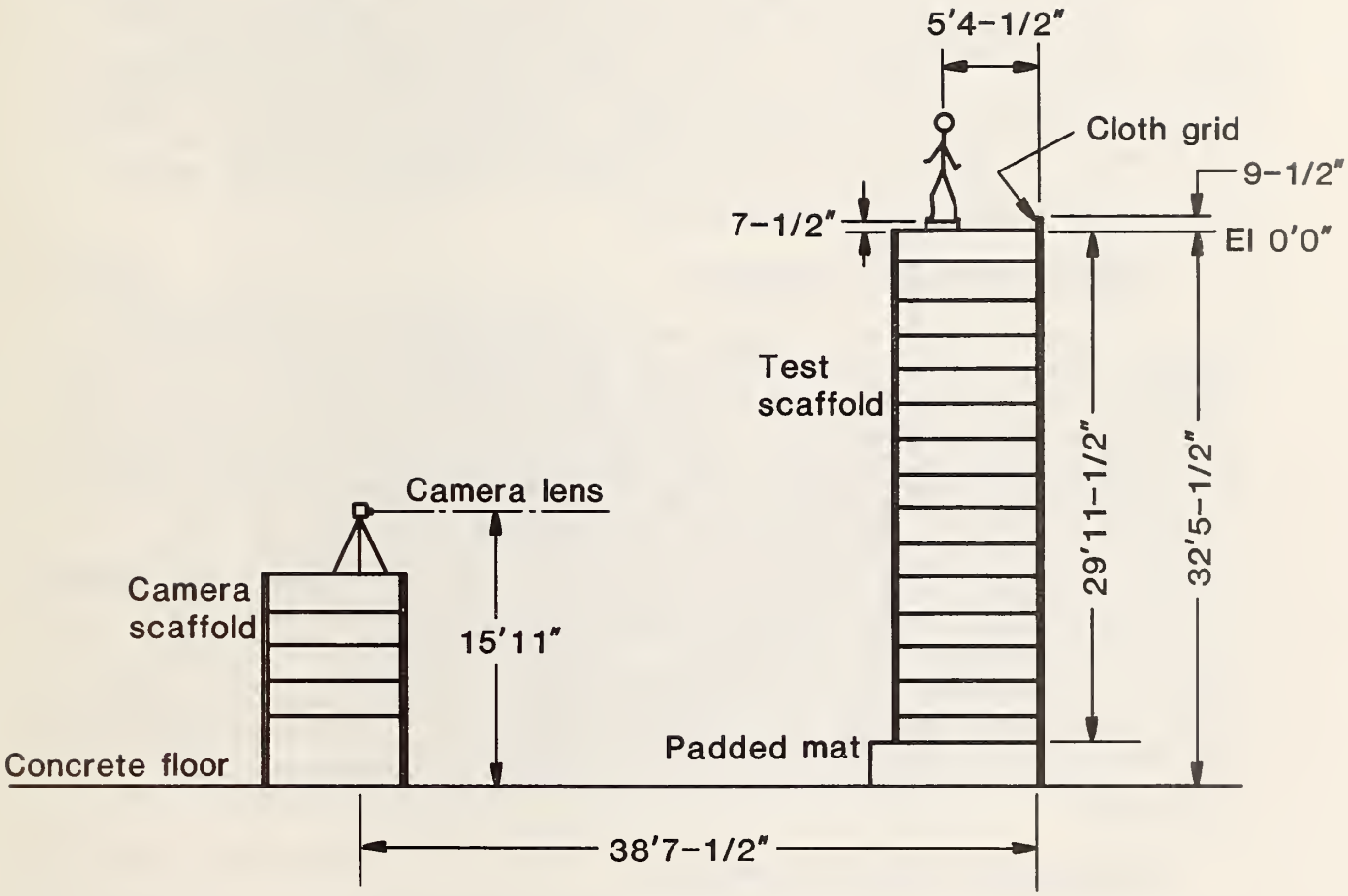

Figure 2.5 Elevation view of test and camera scaffolds

2.4.2 Correction for Vertical Parallax in Photographs

Due to the changing vertical position of the test dummies relative to the position of the camera, there was a built-in distortion (parallax)in the photographs. As illustrated in figure 2.6, the lens of the camera was positioned at approximately the same elevation as the center height of the grid. Thus, when a point on the falling body (e.g. the c.g.) was at any elevation other than that of the grid's center point, it appeared on the photograph to be higher or lower than its actual elevation. Because of this vertical parallax, the measurements of vertical position obtained from photographs, had to be corrected. Figure 2.6 shows the geometric relationship between the actual and apparent positions of the falling body. The derivation of the correction equation is also given.

2.5 SUMMARY OF TEST PROCEDURE

Prior to each test, the dummy was hoisted into an upright position near the leading edge of the trolley using an overhead crane. Once the dummy was stabilized atop the trolley the cylinder's piston was fully retracted to its starting position. Then the pressure regulator was set for the desired air pressure. A countdown was initiated by the operator of the cylinder's solenoid switch to synchronize the initial movement of the trolley with the starting of the camera's motor drive. The trolley assembly rolled along the 20-in (0.5-m) long track until it hit the metal stop and the dummy was propelled over the unguarded edge of the platform. Discrete points along the dummy`s trajectory were photographically recorded. Once the dummy had come to rest on the mat, the horizontal distance from the edge of the scaffold to the farthest point on the dummy's body (usually at the bottom of the feet) was measured and recorded.

3. PRESENTATION OF TEST RESULTS

3.1 HORIZONTAL DISPLACEMENT OF BODY AT LANDING

A total of 48 simulated fall tests was performed from the elevated platform to obtain data on the maximum horizontal movement of falling bodies. There were four tests variables: 1) size of dummy - 95th and 50th percentile, 2) orientation of dummy before falling (i.e., facing unguarded edge, back to unguarded edge and side to unguarded edge, 3) air pressure in the cylinder - 80 and 40 psi, and 4) vertical position of the pneumatic cylinder (i.e., at ankle level and at the approximate level of the center of gravity of the 95th percentile dummy). The distribution of the tests across these variables is shown graphically in figure 3.1.

d = Distance between dummy & screen

P_i = Point on dummy at position 1

Δ_i = Actual drop distance

δ_i = Apparent drop distance

X = Distance between camera & grid

h = Distance from reference point to to ℄ of lens

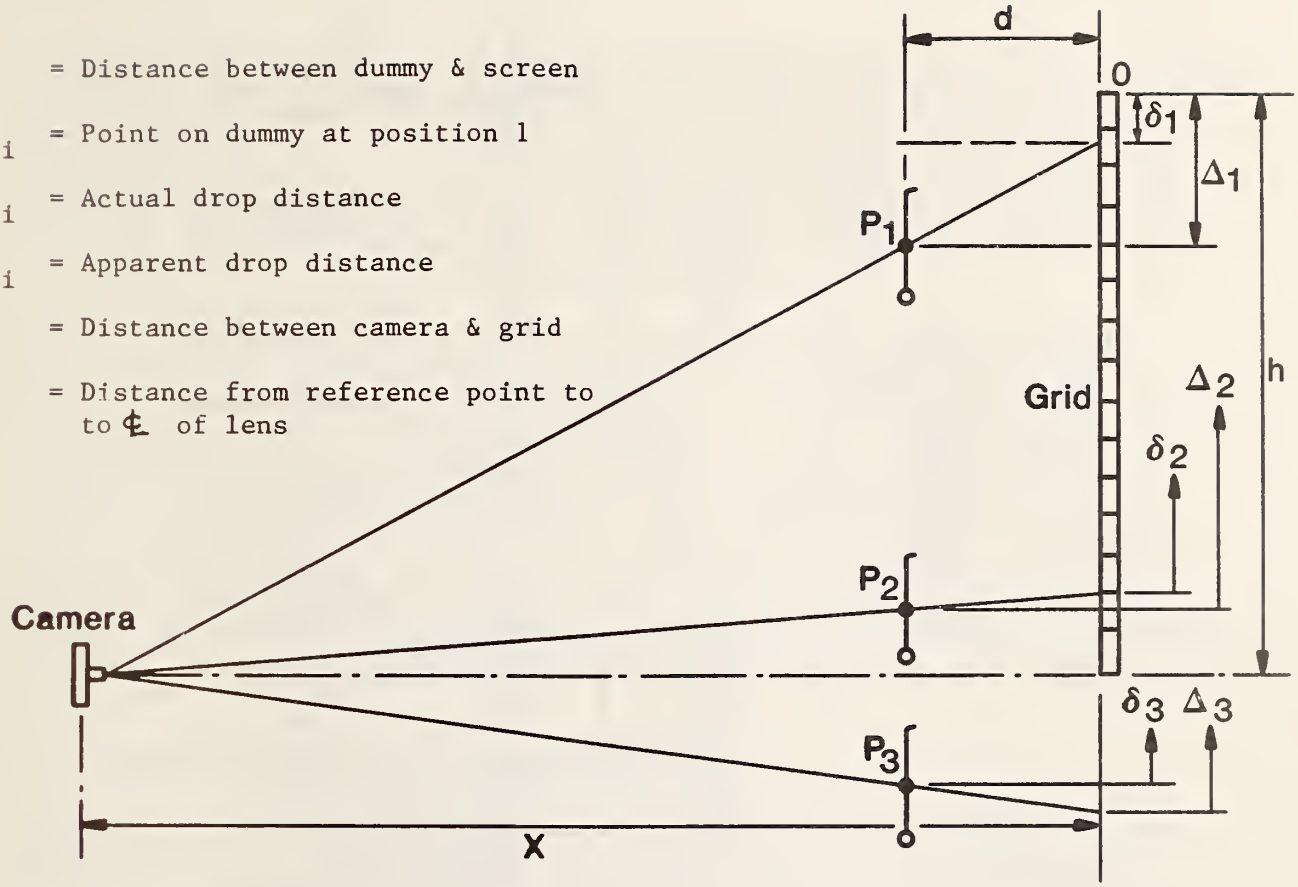

From Similar Triangles:

$$\frac{\Delta - \delta}{d} = \frac{h - \delta}{X}$$

From Points Above the ℄ :

$$\Delta - \delta = d \left(\frac{h - \delta}{X}\right) = E$$

From Field Measurements:

d = 5.375'
h = 15.79'
X = 38.60'

$$E = \frac{5.375}{38.60} (15.79 - \delta) = (0.1391)(15.79 - \delta)$$

$$\Delta = \delta + E = \delta + 0.139 (15.79 - \delta)$$

$$\Delta = (1 - 0.139)\delta + 2.195$$

$$\Delta = 0.861\delta + 2.195$$

This correction equation can be used for body positions above or below the ℄ .

Figure 2.6 Correction for vertical parallax

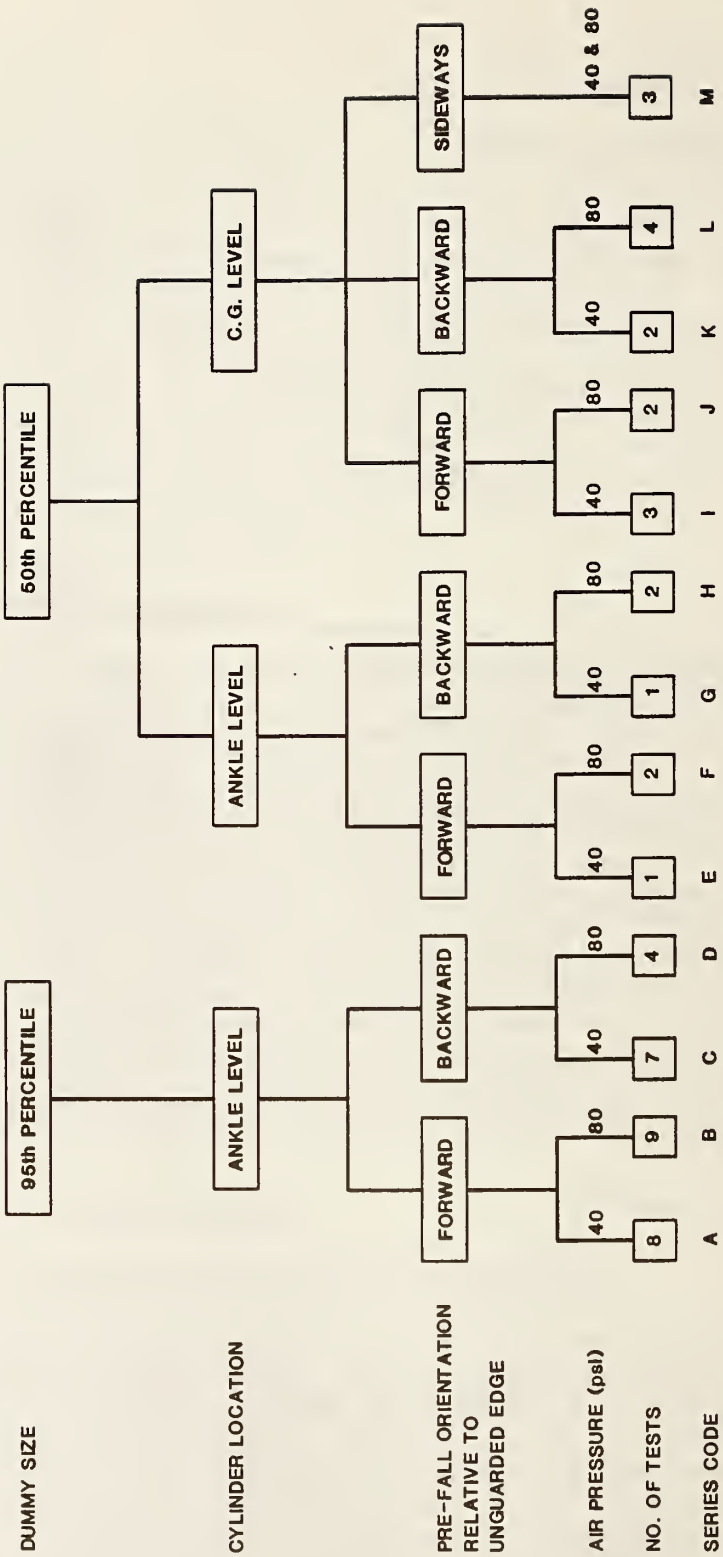

Figure 3.1 Distribution of simulated fall tests

It should be noted that the two different pressures were selected to obtain two significantly different horizontal velocities (2.5 and 1.25 fps) of the dummies at the time of departure from the platform. However, as was discussed in section 2.4, the ratio of the measured velocities was considerably smaller than the 2 to 1 ratio of cylinder pressures. The measured departure velocities were 2.0 and 1.7 fps (0.61 and 0.52 m/s).

The horizontal distance of the dummies in the final landing positions are summarized in table 3.1. The individual test and series average measurements are given in columns (5) and (6) respectively. Where there were three or more tests performed for a series, a standard deviation value is given in the last column. Figure 3.2 illustrates the landing distance to which reference is made in table 3.1. With two exceptions (Series J and L), the average values of the distance from the end of the track to the farthest point on the dummy's body (usually the bottom of the feet) equaled or exceeded 10 ft (3.04 m). Moreover, on eight falls the distance to the farthest point exceeded 12 ft (3.66 m).

3.2 TRAJECTORY OF THE FALLING BODY

Figure 3.3 presents a typical sequence of photographs of the trajectory of a test dummy. The photographs show the descent pattern of the 95th percentile dummy during one of the Series A tests. The photograph in the upper left corner of figure 3.3 was taken just after the trolley had made impact with the metal stop plate. As is illustrated in the upper middle photograph, the dummies first pivoted about their feet until they had fallen to a nearly horizontal position. Then, as shown in the upper right photograph, they were propelled horizontally away from the face of the scaffold. As shown in the remaining photographs of the series, the dummies rotated in air while translating horizontally. In general, they rotated about three-fourths of a full revolution before coming to rest in either a prone or supine position. On several occasions, the dummies underwent almost a full somersault, thereby touching the mat feet first in an almost standing position. They would then rotate back to the mat and come to rest as described above. By observing the lower right photograph in figure 3.3, one can discern that the dummy came to rest in a supine position with the feet farthest from the scaffold.

Figure 3.3 also provides a case-in-point for illustrating the graphical procedure used to determine discrete positions of each dummy's center of gravity during descent. Enlargements were made of each negative frame containing the test dummy in descent and the dummy's center of gravity was identified on each photograph. It was observed in obtaining the measurements listed in table 2.1 that along the length of each dummy's body the center of gravity fell on an imaginary transverse line passing through the

Table 3.1 Summary of Landing Distance Data

(1) SERIES CODE	(2) TEST NUMBER[1]	(3) DUMMY DESCRIP-TION	(4) DEPARTURE VELOCITY (fps)	(5) LANDING[2] DISTANCE (ft)	(6) AVERAGE LANDING DISTANCE (ft)	(7) STANDARD DEVIATION (ft)
A	3-27-4-3	95th	1.7	11.92	11.80	0.89
	3-29-4-1			12.17		
	3-30-4-1			12.25		
	3-30-4-2			12.42		
	3-30-4-3			12.75		
	3-30-4-4			12.25		
	12-12-3-1			10.67		
	10-16-4-1			10.00		
B	12-9-3-1	95th	2.0	10.92	10.94	0.64
	12-9-3-2			10.58		
	12-9-3-3			10.33		
	12-9-3-4			11.00		
	3-4-4-1			10.83		
	3-5-4-1			10.42		
	3-27-4-1			12.00		
	3-27-4-2			10.42		
	10-22-4-1			12.00		
C	3-29-4-2	95th	1.7	11.25	10.75	0.87
	4-4-4-1			12.25		
	4-4-4-3			10.83		
	4-4-4-4			10.83		
	4-5-4-1			10.58		
	3-30-4-5			9.67		
	11-7-4-2			9.67		
D	4-6-4-1	95th	2.0	10.83	10.25	0.96
	4-6-4-2			11.17		
	11-1-4-1			9.00		
	11-7-4-1			10.00		
E	11-8-4-4	50th	1.7	10.67	10.67	-
F	11-7-4-3	50th	2.0	11.75	10.83	-
	11-8-4-1			9.92		
G	11-8-4-5	50th	1.7	10.33	10.33	-

1. The test number are coded according to the date on which the number of tests run on that date. For example test no. 11-7-4-4 refers to the 4th test run on Nov. 7, 1984.

2. Refer to figure 3.2.

Table 3.1 Summary of Landing Distance Data (Continued)

SERIES CODE	TEST NUMBER[1]	DUMMY DESCRIP-TION	DEPARTURE VELOCITY (fps)	LANDING[2] DISTANCE (ft)	AVERAGE LANDING DISTANCE (ft)	STANDARD DEVIATION (ft)
H	11-7-4-4	50th	2.0	11.42	11.62	-
	11-8-4-3			11.83		
	12-4-4-4			8.83		
I	12-5-4-2	50th	1.7	9.83	10.08	1.39
	12-5-4-3			11.58		
J	12-3-4-1	50th	2.0	8.83	8.75	-
	12-3-4-3			8.67		
K	12-5-4-1	50th	1.7	10.75	10.96	-
	12-5-4-4			11.17		
	12-4-4-3			10.75		
	12-3-4-2			9.25		
L	12-4-4-1	50th	2.0	9.17	9.56	0.79
	12-4-4-2			9.08		
	12-5-4-6		1.7	8.17		
M	11-8-4-2	50th	2.0	11.92	10.42	1.98
	11-8-4-6		1.7	11.17		

[1] The test numbers are coded according to the date on which the number of tests run on that date. For example test no. 11-7-4-4 refers to the 4th test run on Nov. 7, 1984.

[2] Refer to figure 3.2.

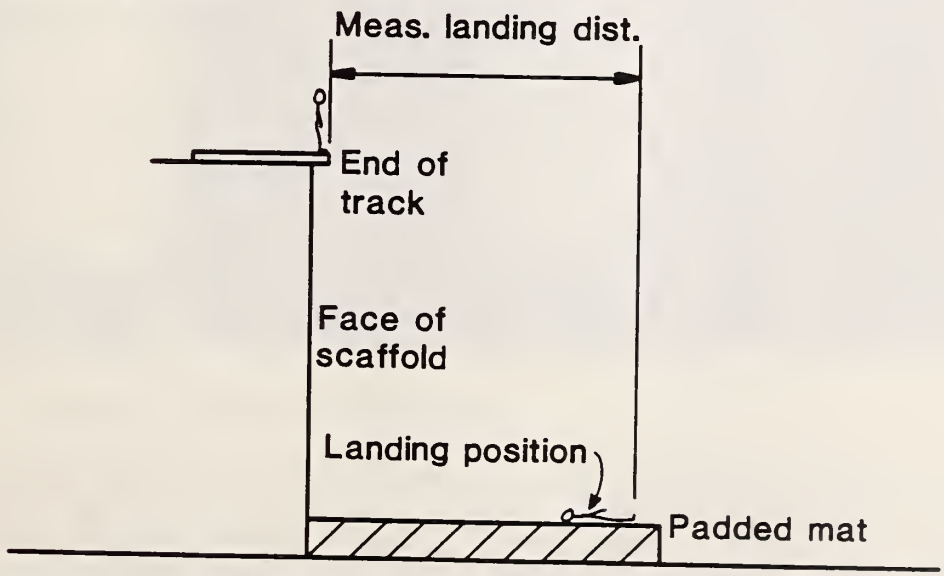

Figure 3.2 Description of measured landing distance

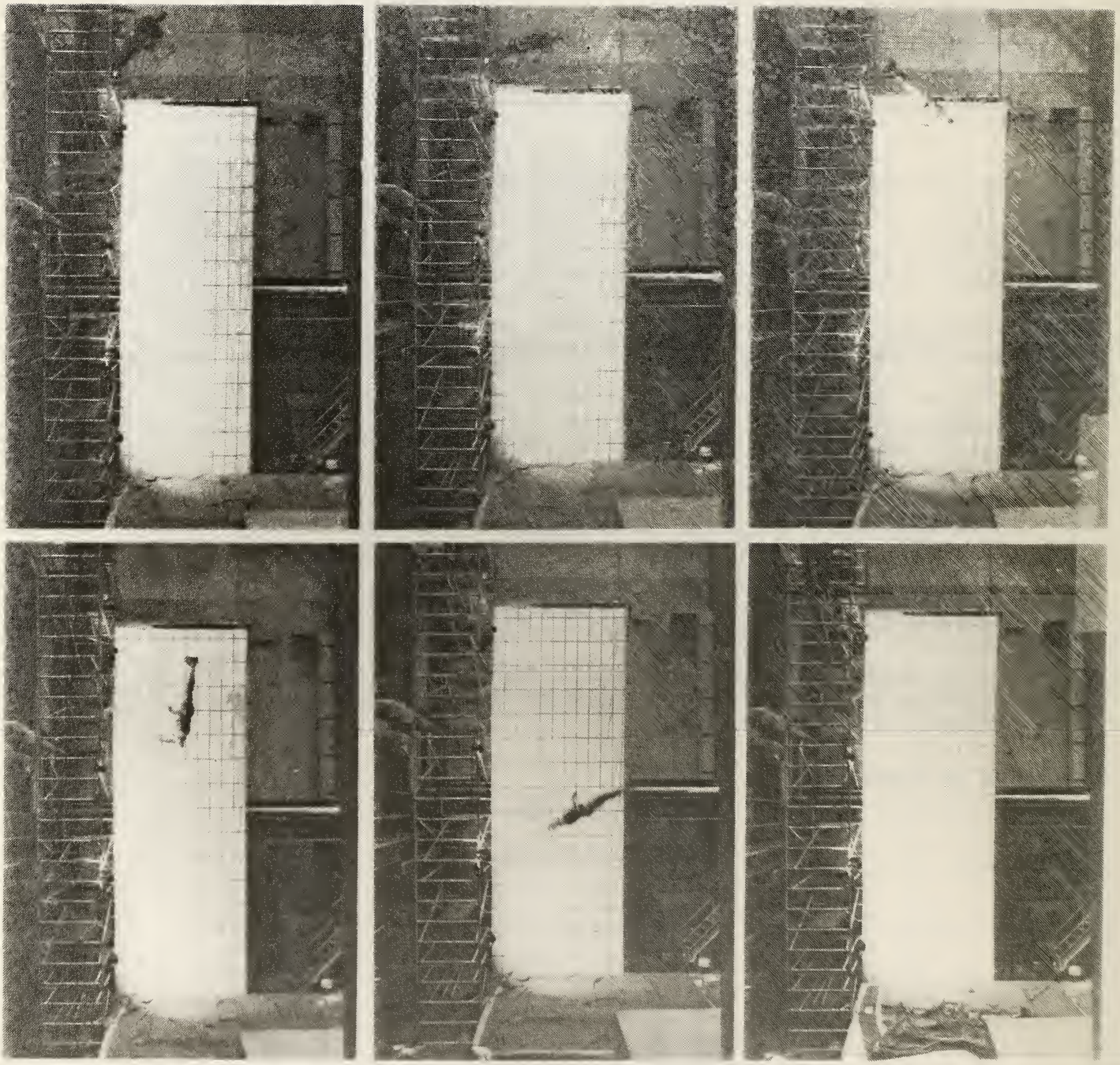

Figure 3.3 Typical trajectory of test dummy

middle of the buttocks. This observation became the basis for the guideline for locating the center gravity on the side of a dummy in each photograph.

The respective center of gravity positions were referenced to the grid pattern in the background of the photograph and the coordinates were recorded. Corrections were made to the vertical measurements to compensate for the parallax due to the relative elevations of the falling body and the lens of the camera as described in section 2.5. Also, corrections were made to the horizontal excursion measurements to account for horizontal parallax.

4. ANALYSIS OF FALL TRAJECTORY

4.1 INTRODUCTION

Analysis of the motion of the dummy during the tests can be separated into 5 stages:

1. Horizontal translation with constant initial velocity, .
2. Transformation from translational motion to rotational motion when trolley impacts the rigid stop.
3. Rotation about its feet.
4. Departure from platform.
5. Free fall.

In order to perform a parametric study of fall trajectories, an analytical model was developed for predicting fall trajectories for different initial conditions. This chapter describes the analytical model and compares predicted fall trajectories with measured values.

4.2 ANALYTICAL MODEL

The human body is a complex assemblage of rigid members, such as arms and legs, and it would be difficult to develop an accurate kinematic model to describe the motion of the center of gravity and of the various members. For the purpose of this study a simple model was used to predict the motion of the center of gravity of the dummy. It is assumed that the dummy can be represented by a long slender rod of weight W and length . The equations describing the motion of the rod during the stages discussed in the previous section are given below.

4.2.1 Initial Angular Velocity

The rod is assumed to be moving with a constant initial horizontal velocity of V_{hi} (figure 4.1 (a)). The translational motion of the rod is stopped by a small rigid stop. This is to simulate the sudden stopping of the trolley when it impacts the rigid plate at the end of the track. The impact causes the rod to change its

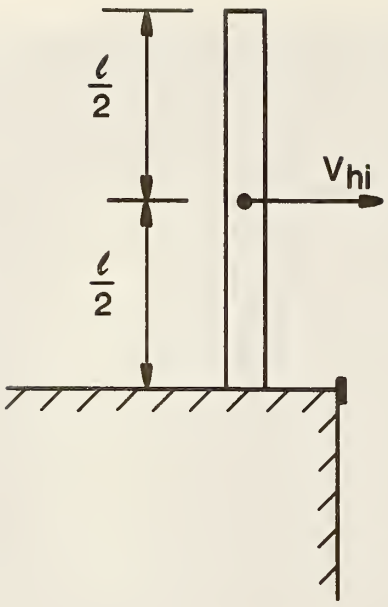

a) Translation

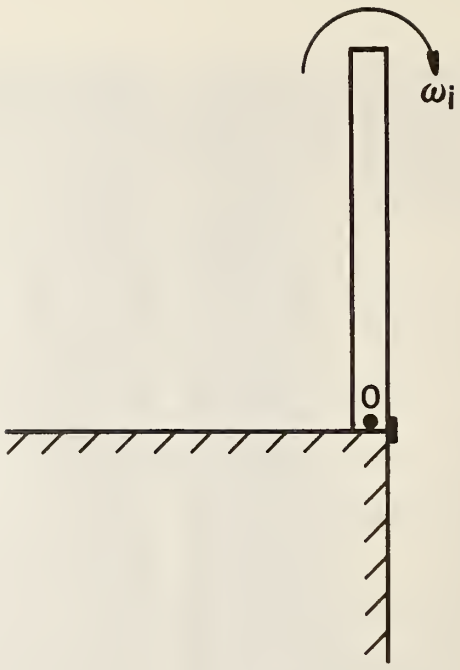

b) Impact

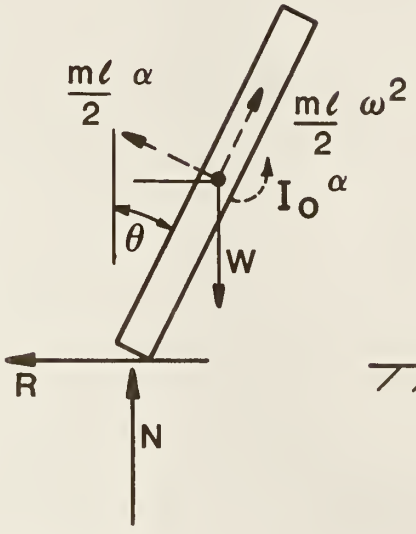

c) Free body diagram

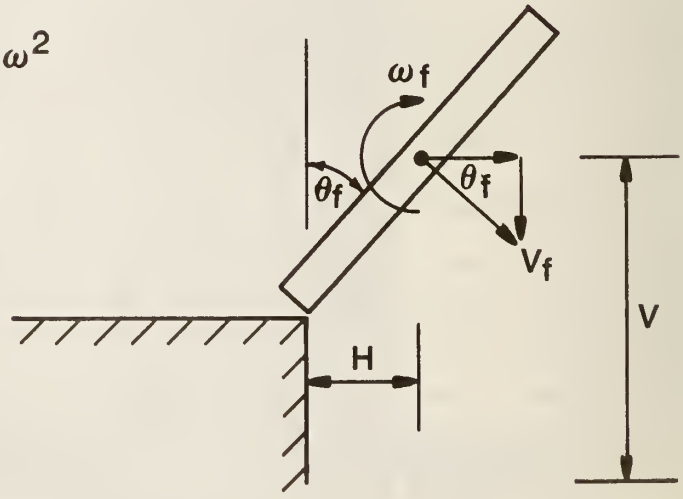

d) Start of free-fall

Figure 4.1 Analytical rod model

motion from pure translation to rotation about its bottom end. The angular velocity at the instant after impact may be computed by applying the principle of conservation of angular momentum about point 0 (see figure 4.1.b). First, the moment about 0 of the linear momentum H_i, is computed.

$$H_i = mv_{hi} \frac{\ell}{2} \tag{4.1}$$

After the impact the rod has an angular velocity α_i and the angular momentum about 0, H_o, is:

$$H_o = I_o \omega_i \tag{4.2}$$

where I_o = mass moment of inertia about point 0 (= 1/3 m ^{2})

By equating (4.1) and (4.2), the initial angular velocity ω_i, is:

$$\omega_i = \frac{mv_{hi}\ell}{2I_o} \tag{4.3a}$$

$$\omega_i = \frac{3v_{hi}}{2\ell} \tag{4.3b}$$

4.2.2 Rotation About Fixed End

After the forward motion of the trolley was stopped, the dummies rotated about their feet. During the course of the rotational motion, the dummies slid off the platform. Sliding occurred when the external and inertial forces surpassed the sliding resistance beneath the dummies' feet. Thus, the forces acting on the rod model as a function of the angle of rotation must be calculated.

Figure 4.1 (c) is a freebody diagram of the rod showing the external forces as solid lines and the inertial forces as dashed lines. The inertial forces arise from the normal and tangential accelerations of the center of gravity. By equating forces in the horizontal and vertical directions, the following expressions for the normal (N) and horizontal (R) reactions acting at point 0 are obtained.

$$N = W - m \frac{\ell}{2} (\alpha \sin\theta + \omega^2 \cos\theta) \tag{4.4}$$

$$R = m \frac{\ell}{2} (\omega^2 \sin\theta - \alpha \cos\theta) \tag{4.5}$$

where, W = weight
g = acceleration due to gravity
α = angular acceleration

Sliding occurs when the horizontal force, R, equals the sliding resistance; that is,

$$R = \mu N \tag{4.6}$$

where, μ = coefficient of friction

To determine the angular position of the rod when sliding occurs, it is necessary to determine the angular velocity and angular acceleration as functions of the rotation angle. The angular acceleration is determined by equating the moment of W about point 0 to the time rate of change of the angular momentum about the same point.

$$W \frac{\ell}{2} \sin\theta = I_o \alpha \tag{4.7a}$$

$$\alpha = \frac{3}{2} \frac{g}{\ell} \sin\theta \tag{4.7b}$$

The angular velocity is determined by integration of Eq. (4.7b) and applying the boundary condition that for $\theta = 0^o$ the angular velocity has the initial value given by Eq. (4.3b). Alternatively, the angular velocity may be computed by using the principle of conservation of energy. The latter approach is used. When the rotation angle is 0^o, the rod has a rotational kinetic energy given by

$$KE_i = \frac{1}{2} I_o \omega_i^2 \tag{4.8}$$

As the rod rotates to an angle θ, there is a decrease in the potential energy of the center of gravity, which is given by

$$\Delta PE = mg \frac{\ell}{2} (1 - \cos\theta) \tag{4.9}$$

The decrease in potential energy causes an increase in rotational kinetic energy. Thus,the kinetic energy is

$$\frac{1}{2} I_o \omega^2 = \frac{1}{2} I_o \omega_i^2 + mg \frac{\ell}{z} (1 - \cos\theta) \tag{4.10}$$

Therefore, the angular velocity becomes

$$\omega = [\omega_i^2 + \frac{3g}{\ell} (1 - \cos \theta)]^{1/2} \qquad (4.11)$$

By substituting Eqs 4.7 (b) and 4.11 into Eqs. 4.4 and 4.5 and by applying the condition given by Eq. 4.6, the angular orientation of the rod can be determined when sliding occurs. By substituting this angle into Equation 4.11, the angular velocity at sliding is determined.

4.2.3 Fall Trajectory

It is assumed that when sliding occurs, the rod leaves the platform and undergoes free-fall. The initial velocity, V_f, at the start of free-fall is

$$V_f = \frac{\ell}{2} \omega_f \qquad (4.12)$$

Where ω_f is the angular velocity when sliding occurs. The velocity V_f is directed at the angle θ_f, so that the center of gravity has vertical and horizontal velocity components (see figure 4.1 (d)):

$$V_v = V_f \sin \theta_f \qquad (4.13)$$

$$V_h = V_f \cos \theta_f \qquad (4.14)$$

The position (H,V) of the center of gravity may now computed.

$$H = \frac{\ell}{2} \sin \theta_f = V_h t \qquad (4.15)$$

$$V = h + \frac{\ell}{2} \cos \theta_f - V_v t - \frac{1}{2} g t^2 \qquad (4.16)$$

where, h = height of platform
t = time from the start of sliding

The vertical position is referenced with respect to ground level and the horizontal position is referenced with respect to the edge of the platform. The angular orientation of the rod, during free-fall can be determined by adding the product ω_f x t to the angle θ_f.

4.2.4 Parametric Study

The analytical model requires the following input parameters: initial velocity, V_{hi}; length of rod, ; weight of rod, W ; and coefficient of friction, μ. Of these, only the coefficient is not known. Hence, the effects of the coefficient of friction on the computed fall trajectory were studied. The governing equations given in the previous section were programmed into a computer and the trajectories were computed for different values of coefficient of friction. Figure 4.2 shows the positions of the rod at 0.1 -second increments for coefficients of friction varying from 0.1 to 0.9. Time is measured from the instant of sliding. The quantities "Height" and "Distance" represent the location of the center of gravity at the last time step. The "take-off angle" is the angular position of the rod when sliding occurs (i.e., θ_f). It is seen that a wide variation in the coefficient of friction results in a negligible effect on the trajectory.

Fall trajectories were computed for different rod lengths (approximately equivalent to heights of people) to determine the sensitivity of trajectory to different heights of people. Figure 4.3 shows the rod positions at different time steps as the rod length was varied from 6.5 ft (2.0 m) to 4.5 ft (1.4 m). The quantity "CG" is the distance from the lower end of the rod to its center of gravity, which in this case is one-half the rod length. It is seen that a reduction in rod length has a significant effect on the fall trajectory; the horizontal distance from the edge of the platform to the center of gravity of the rod at rest decreases with decreasing rod length while the cumulative angular rotation at impact increases. The results of the CG Parameter Study can be used to qualitatively account for the possible shift in the position of the center of gravity during a dummy's approach to the edge of the platform. The location of the center of gravity can be practically measured only while a dummy is in the erect stationary orientation. However, it is possible that the relative positions of the limbs and torso can change prior to the start of sliding and hence the vertical position of the center of gravity can change. The qualitative effect of this shifting center of gravity can be inferred from the results of the CG Parameter Study.

So far in the analysis, it has been assumed that free-fall starts when sliding occurs. Physically, this means that the rod is at the edge of the platform when sliding starts (see figure 4.4). However, it is possible to stop the horizontal translation of the

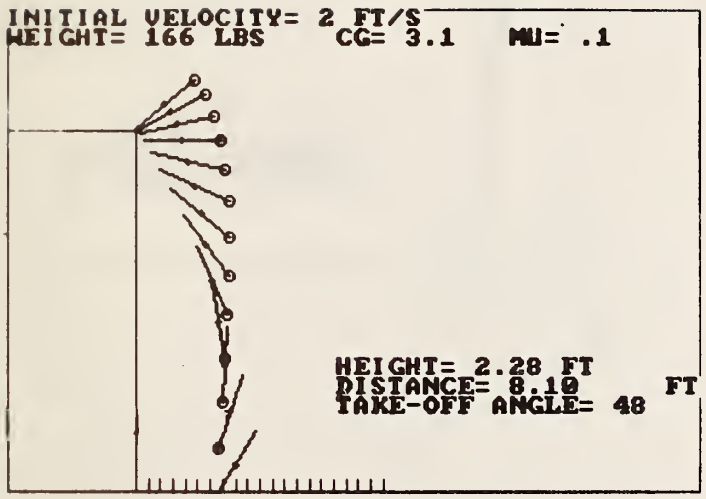

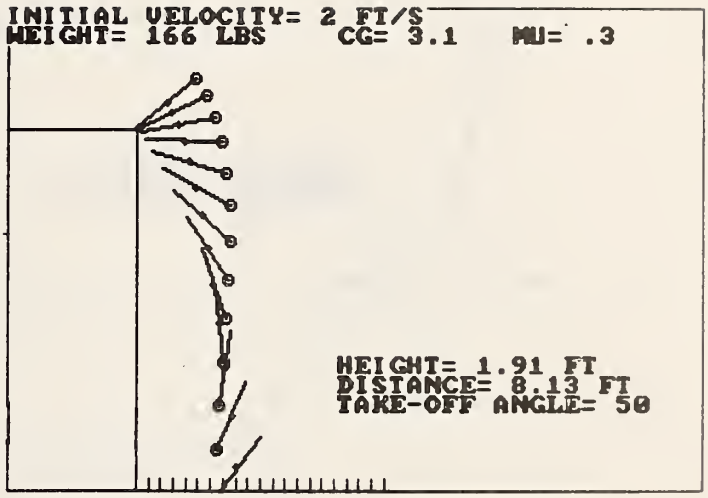

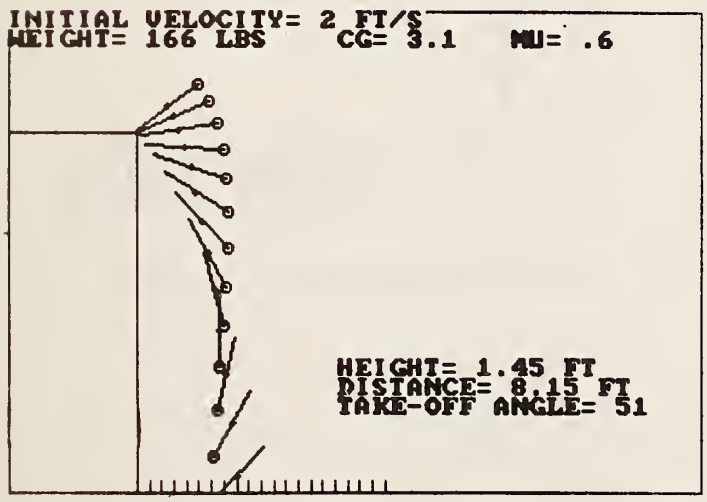

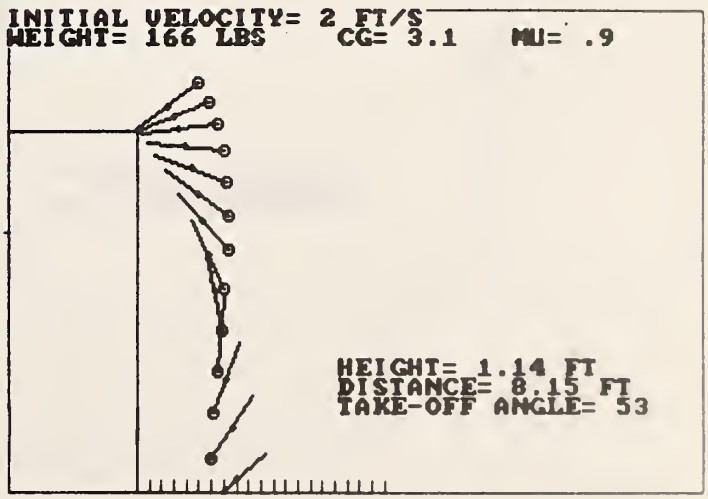

Figure 4.2 Effect of coefficient of friction on computed fall trajectories.

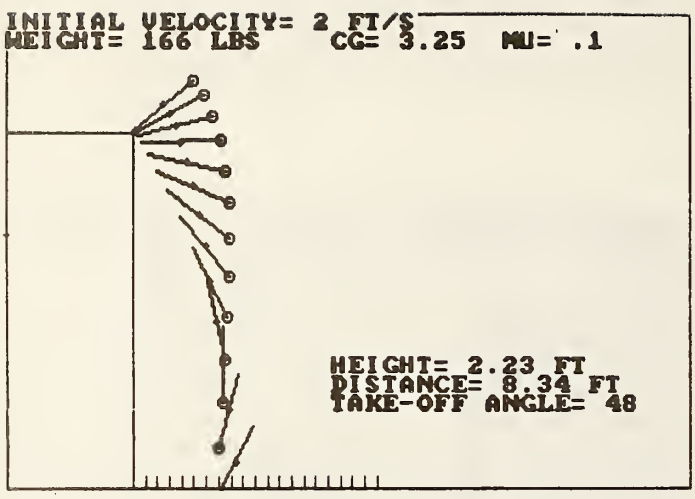

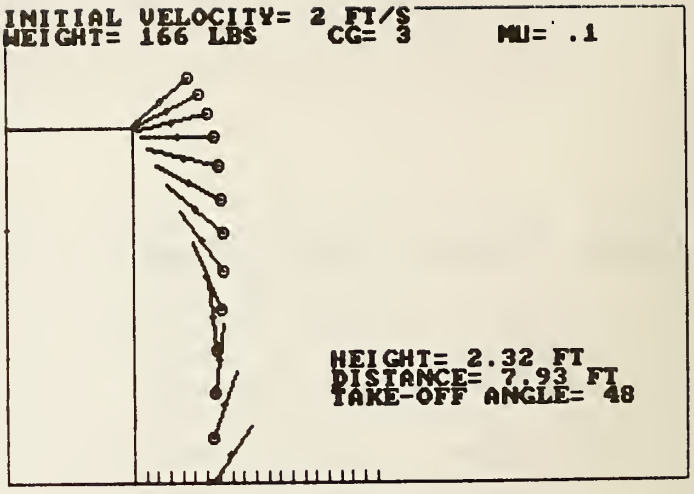

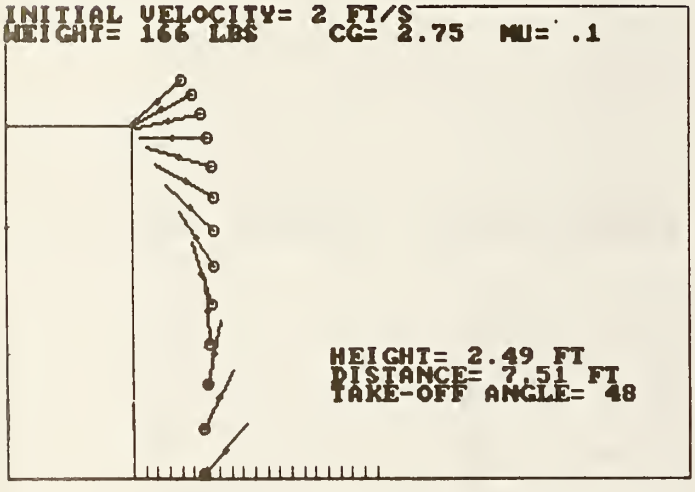

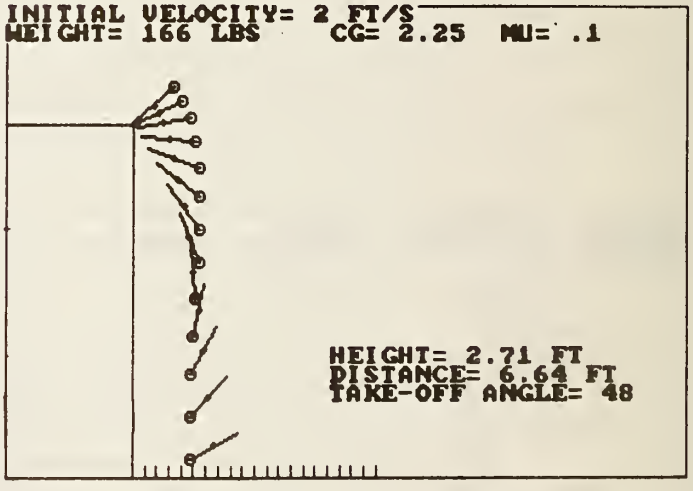

Figure 4.3 Effect of height of center of gravity on computed fall trajectories.

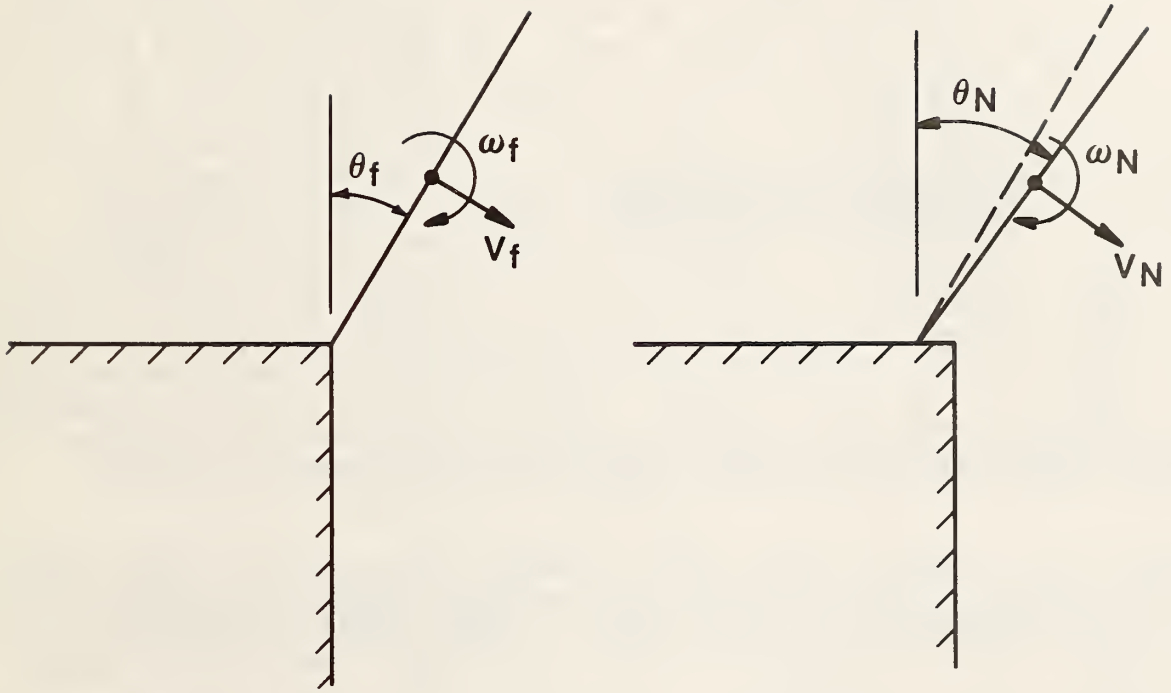

a) Sliding R = μN

b) Lift-off N = 0

Figure 4.4 Conditions at start of free-fall

rod at a point before the platform edge. In this case the start of sliding does not result in free-fall until either: 1) the rod slides off the platform or 2) the rod lifts-off the platform. The rod can lift off the platform because the normal force given by Eq. 4.4 can become equal to zero as the angle θ increases. This lift-off condition is analogous to a diver lifting off from a diving board. Rigorous analysis of these two conditions is rather difficult as it would be necessary to consider energy losses due to sliding friction. For this study a simplified approximation was used. It was assumed that a limiting condition would be to consider the case of lift-off without sliding. This simply requires determining the angle θ_n when the normal force, N, as given by Eq. 4.4, equals zero. As shown in figure 4.4 (b) the angle θ_n is greater than θ_f, the angle for the start of sliding. Figure 4.5 (a) shows the fall trajectory for the same initial conditions as in figure 4.2, except that free-fall is assumed to start when lift-off occurs. It is seen that the distance is significantly reduced compared with the case of sliding. In addition, the angular rotation at ground impact increases. Figure 4.6 compares the fall trajectories for initial horizontal velocities varying from 0 to 8 ft/s (2.4 m/s). It is seen that the horizontal fall distance increases with increasing velocity, but the increase is not as dramatic as would be expected. Note that zero initial velocity still produces a large horizontal fall distance. The zero velocity case corresponds to a worker standing at platform's edge, simply losing his balance and falling over the edge (i.e condition 2 in figure 1.2).

Finally, the effect of the rod's weight was studied. Referring to section 4.2.3, it is seen that the only governing equations that involve the weight are those dealing with the start of sliding (or lift-off), that is, Eqs 4.4 to 4.6. A closer examination shows that when Eq. 4.6 is used (or N=0), the weight term can be cancelled from the equation. Thus, it can be concluded that the fall trajectory is independent of the rod weight.

In summary, these parametric studies show that the fall trajectories of the rod model are affected significantly by the location of the center of gravity and whether free-fall occurs under a "sliding" or "lift-off" condition. The initial horizontal velocity has a lesser influence. When free-fall is considered to occur at the start of sliding, the value of the coefficient of friction has a negligible effect. The fall trajectory is independent of weight. With this understanding, the measured fall trajectories were compared with the predictions of the rod model.

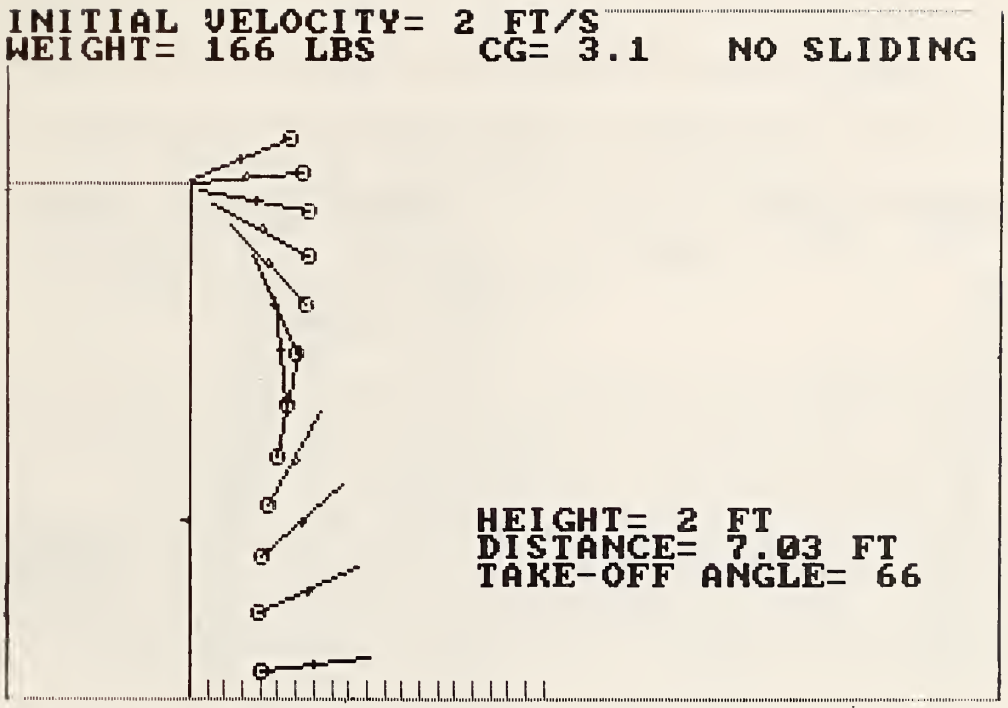

Figure 4.5 a) Fall trajectory under lift-off condition

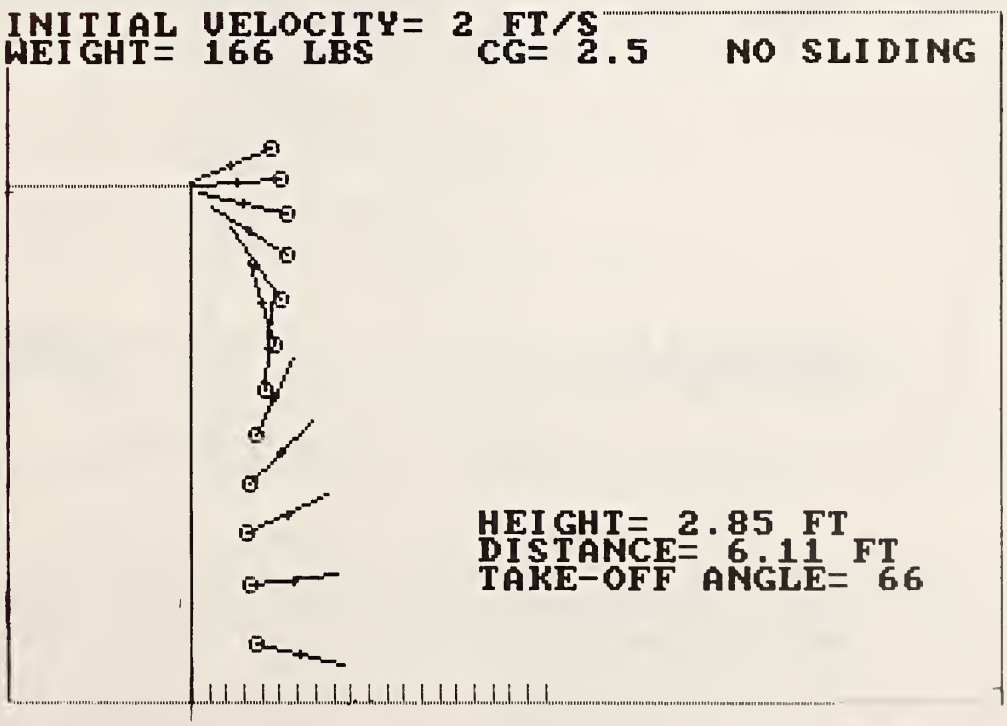

Figure 4.5 b) Fall trajectory with lift-off and reduced height of center of gravity

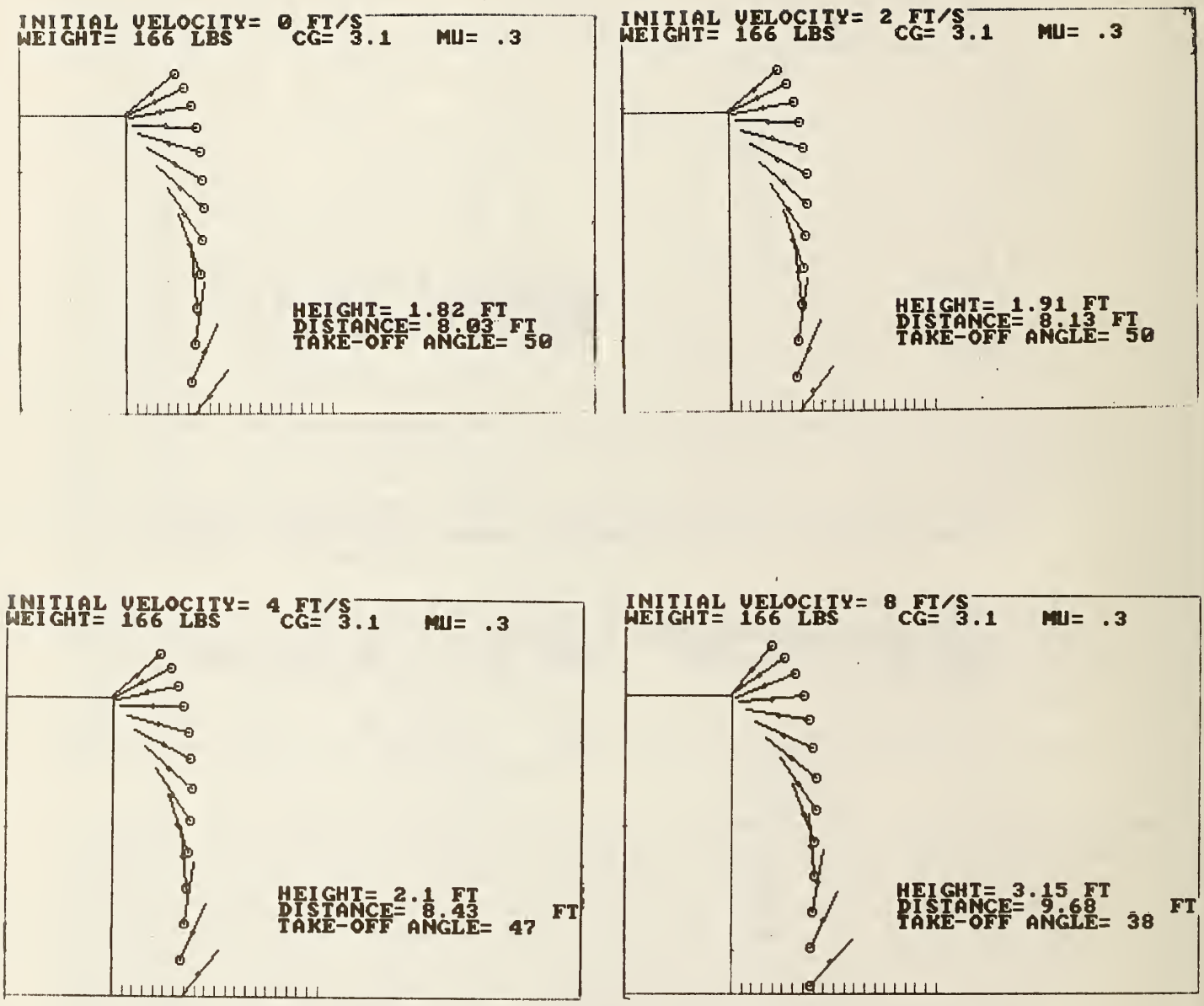

Figure 4.6 Effect of initial horizontal velocity on computed fall trajectories

4.2.5 Comparison of Measured and Computed Trajectories

Chapter 3 described the various testing conditions that were used. As a review, the following variables were studied:

a) size of dummy;
b) air pressure in the loading cylinder;
c) orientation of the dummy; and
d) location of loading cylinder.

The trajectories of the centers of gravity of the dummies were estimated from photographs taken during the free-fall. It was assumed that the location of the center of gravity was at the same point on the dummy, irrespective of the orientation of the legs and arms. However, the photographs indicated movement of the arms and legs during free-fall; this would change the position of the center of gravity. Hence it is estimated that the true X- and Y- coordinate of the center of gravity could lie within plus or minus 1/2-foot (0.15 m) of the values estimated from the photographs.

The experimental results are compared with the predictions from the analytical model to determine whether the model adequately represents the measured trajectories. Since cylinder pressures of 40 and 80 psi (276 and 552 kPa) produced small differences in initial velocity, and since the analytical model indicates that initial velocity does not have a strong effect on the trajectory, the data for the two cylinder pressures were grouped. The results with the 50 percentile dummy are presented first.

Figure 4.7 shows the data for series K and L. The analytical curve is based on the following conditions:

a) coefficient of friction = 0.3
b) initial velocity = 2 ft/s (0.6 m/s)
c) height of center of gravity = 3.1 ft (0.9 m)

Although the model appears to overestimate the horizontal distance to the center of gravity over the upper half of the trajectory, the analytical curve does give a reasonable fit to the data. It should be noted that both the x and y coordinates of the test data points were corrected for parallax.

Figure 4.8 shows the comparison for series I and J. The solid curve is the analytical prediction for the same conditions as in the previous figure. The fit at the lower-half of the trajectory is reasonable; there is more scatter at the upper half. Note that the date for test 12-3-4-3 (Series J) have significantly lower horizontal distances than for the other tests. The dashed line is the analytical solution for the "lift-off" condition. It is seen that the analytical curve moves closer to the data for test

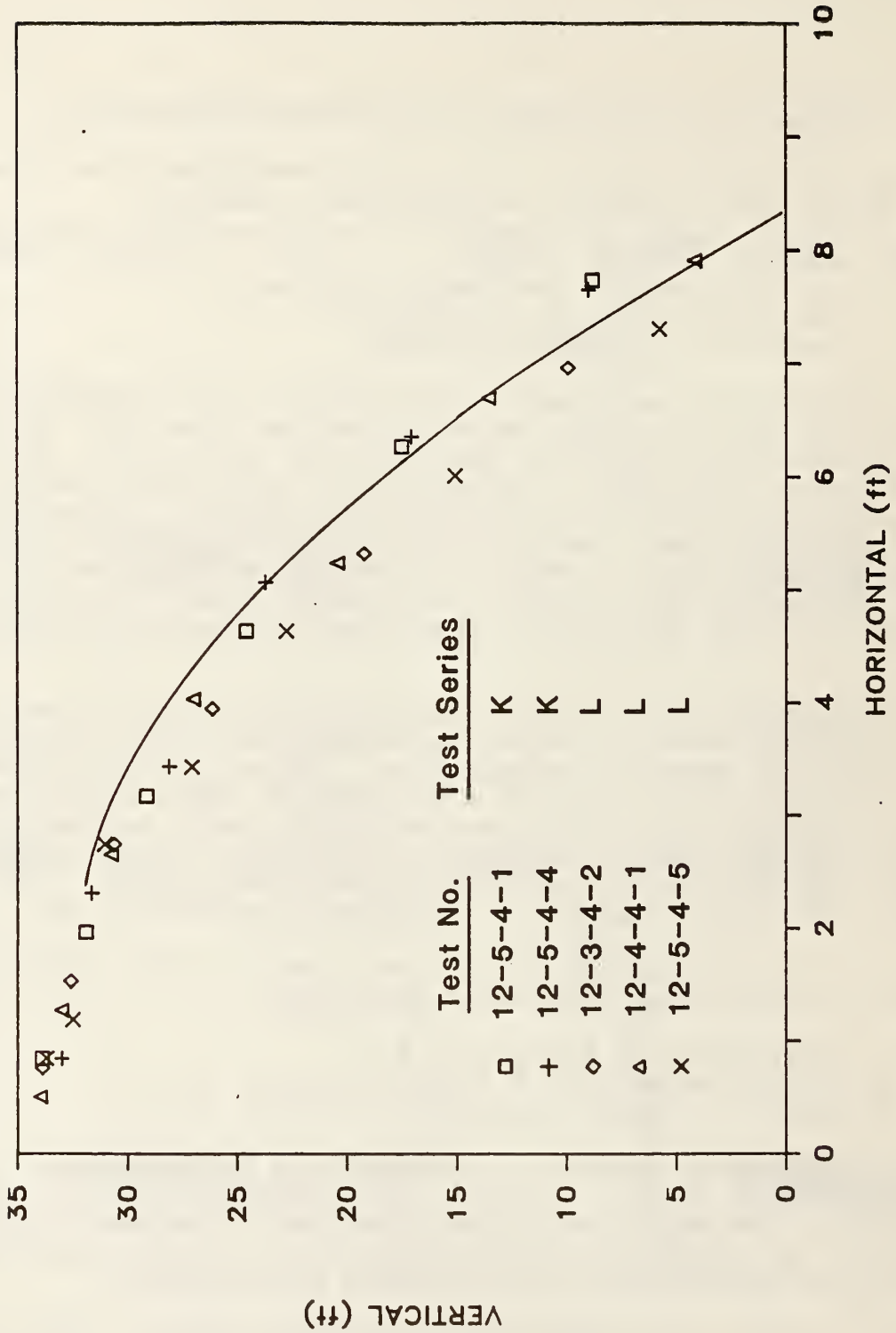

Figure 4.7 Measured locations of center of gravity for series K and L compared with computed trajectory

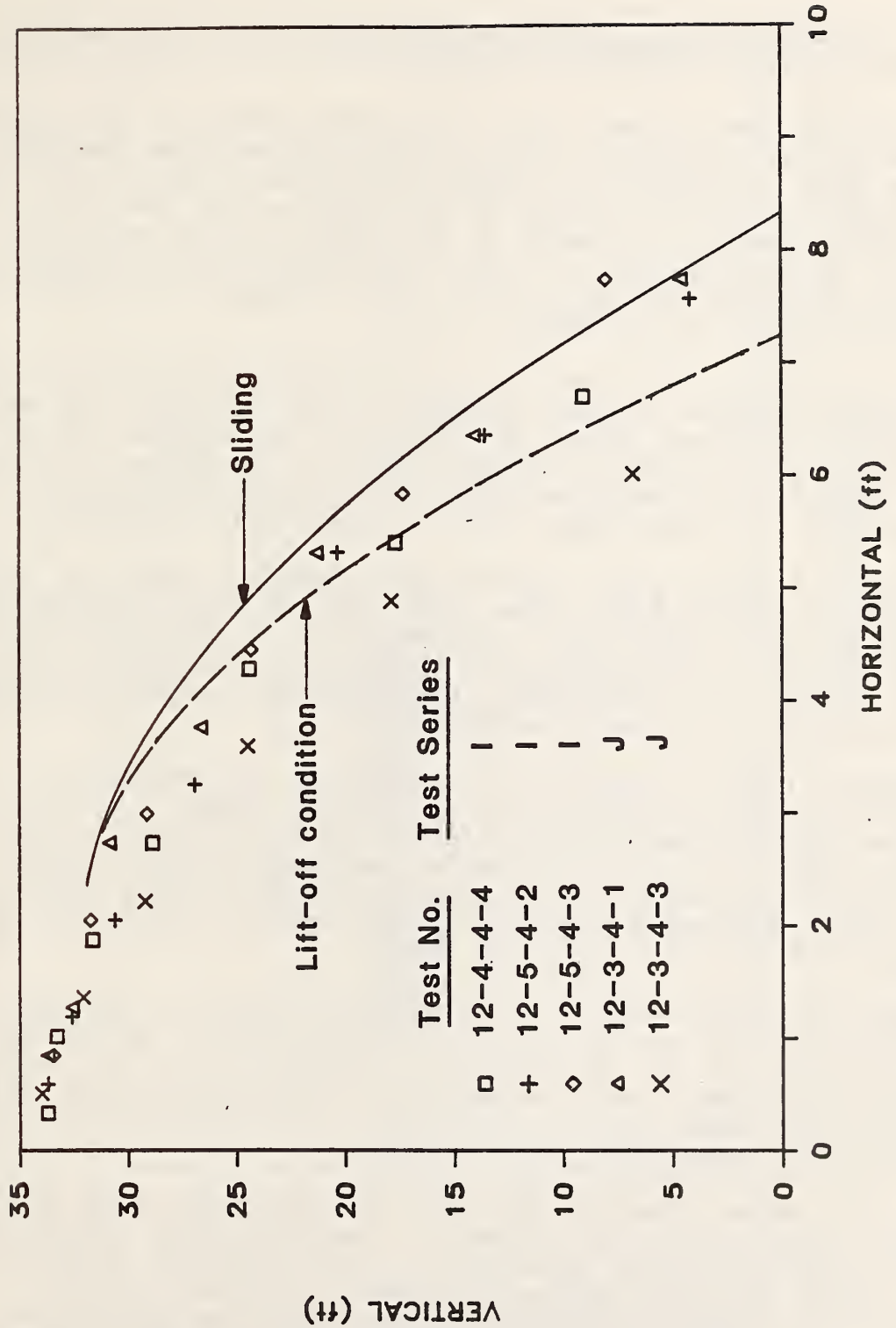

Figure 4.8 Measured locations of center of gravity for series I and J compared with computed trajectory

series 12-3-4-3, but it still over predicts the measured horizontal distance by about 1/2 foot (0.15 m).

Comparing figures 4.7 and 4.8, it is concluded that the pre-fall orientation of the dummy, that is facing forward or backward, does not have a significant effect on the fall trajectory. For these tests series (I through L) the movement of the trolley was produced by pushing the dummy at the level of its center of gravity. By raising the cylinder, the effect of a horizontal force accidentally applied to the back or chest of a worker was produced (Condition 6 in figure 1.2).

Figure 4.9 shows the results for series E,F,G, and H for which the loading cylinder pushed directly on the trolley. The analytical curve is for the same input parameters as in figures 4.7 and 4.8. Again the predicted trajectory is a reasonable fit to the data. Thus, it is concluded that the location of the loading cylinder has no significant effect on the fall trajectory.

In series M the dummy was positioned sideways. The test results are shown in figure 4.10. The solid line is the computed trajectory obtained with the same input parameters as in figures 4.7 through 4.9. The fit is similar to that obtained in the other test series. Thus, it is concluded that placing the dummy sideways did not affect the results significantly.

The dashed lines in figure 4.11 represent the ranges of measured trajectories for the 50 percentile dummy. The data from test 12-3-4-3 have been excluded as it did not fit the overall trends. The solid line is the computed trajectory. From this comparison it is concluded that the simple slender rod model gives reasonable predictions for the fall trajectories of the test with the 50 percentile dummy.

The 95th percentile dummy was in poor mechanical condition compared with that of the 50th percentile dummy. As was mentioned in section 2.2, it was difficult to tighten all of the joints and stabilize the dummy. As a result, the dummy was excessively flexible, and there was some difficulty in performing the tests and obtaining repeatable fall patterns.

Figure 4.12 shows two test results from series A and B in which the 95th dummy was facing forward. The analytical trajectory was based on the same input parameters as for the 50th percentile dummy except that the center of gravity level was 3.4 ft (1.04 m). For this limited data the fit of the calculated trajectory is similar to that obtained with the 50th percentile dummy.

The final comparison is for the 95th percentile dummy facing backward. Figure 4.13 shows the dummy just before departing from the platform during test 11-7-4-1. The dummy was not in an erect

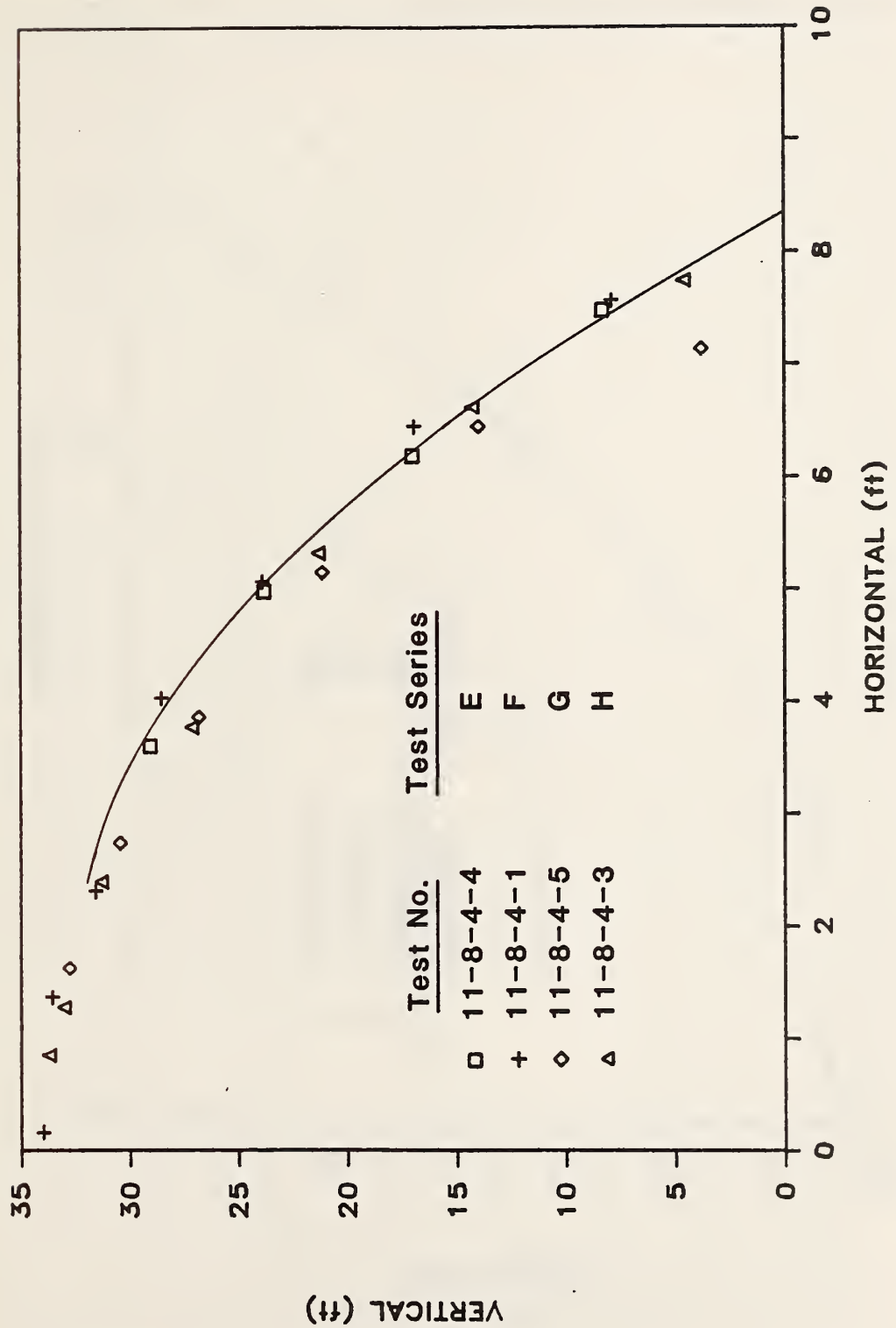

Figure 4.9 Measured locations of center of gravity for series E, F, G, and H compared with computed trajectory

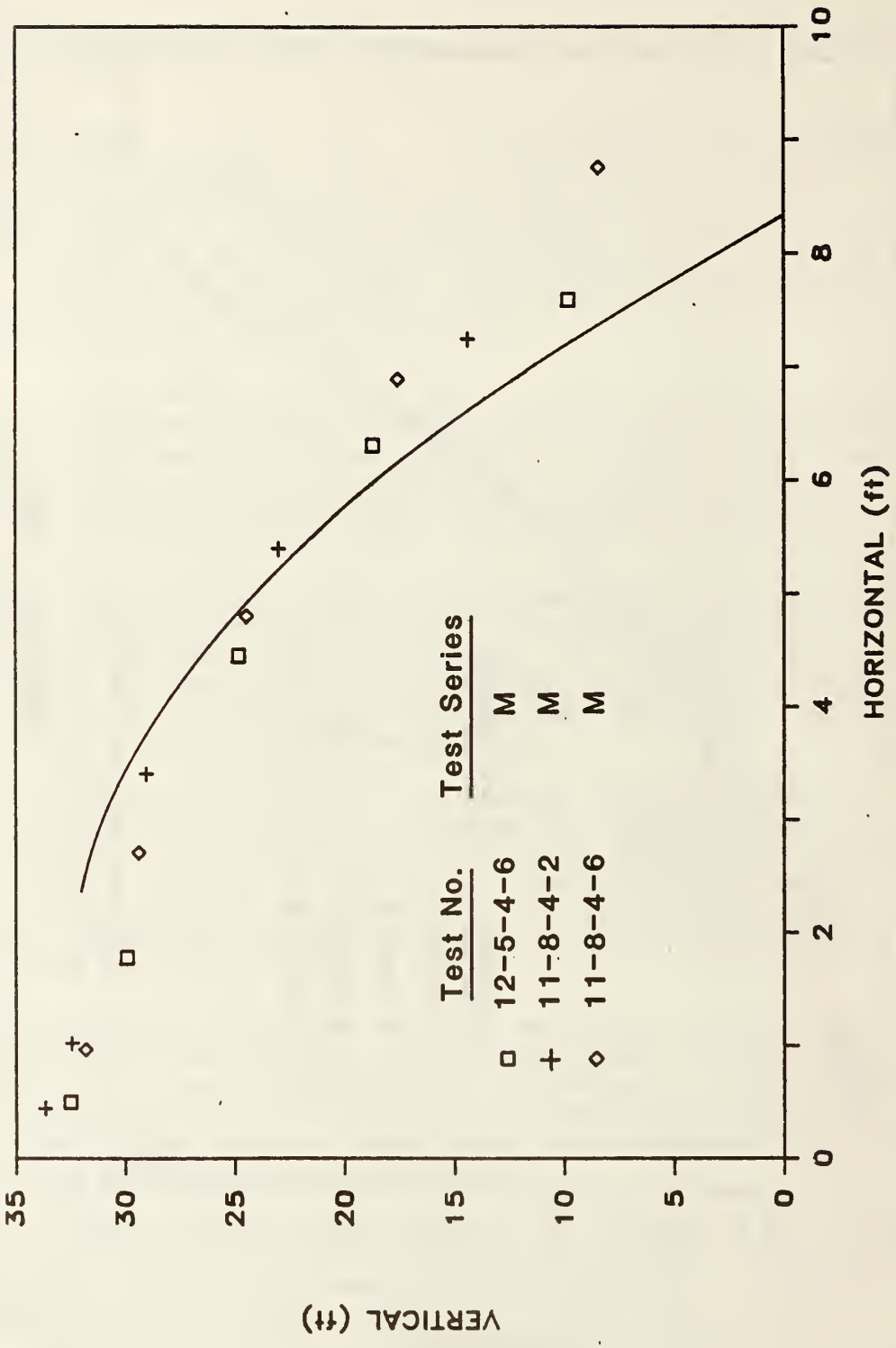

Figure 4.10 Measured locations of center of gravity for series M compared with computed trajectory

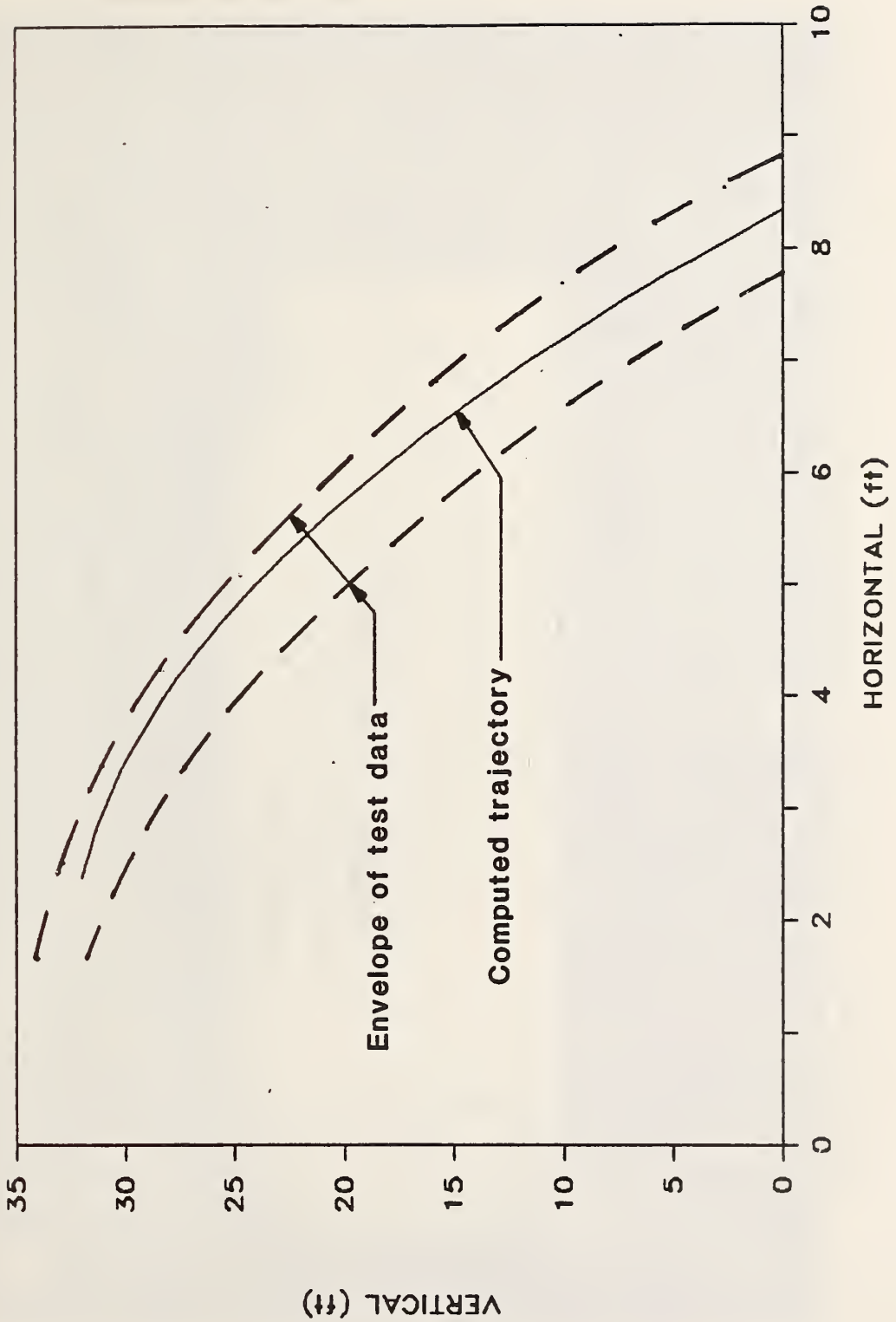

Figure 4.11 Range of measured trajectories for 50th percentile dummy and computed trajectory

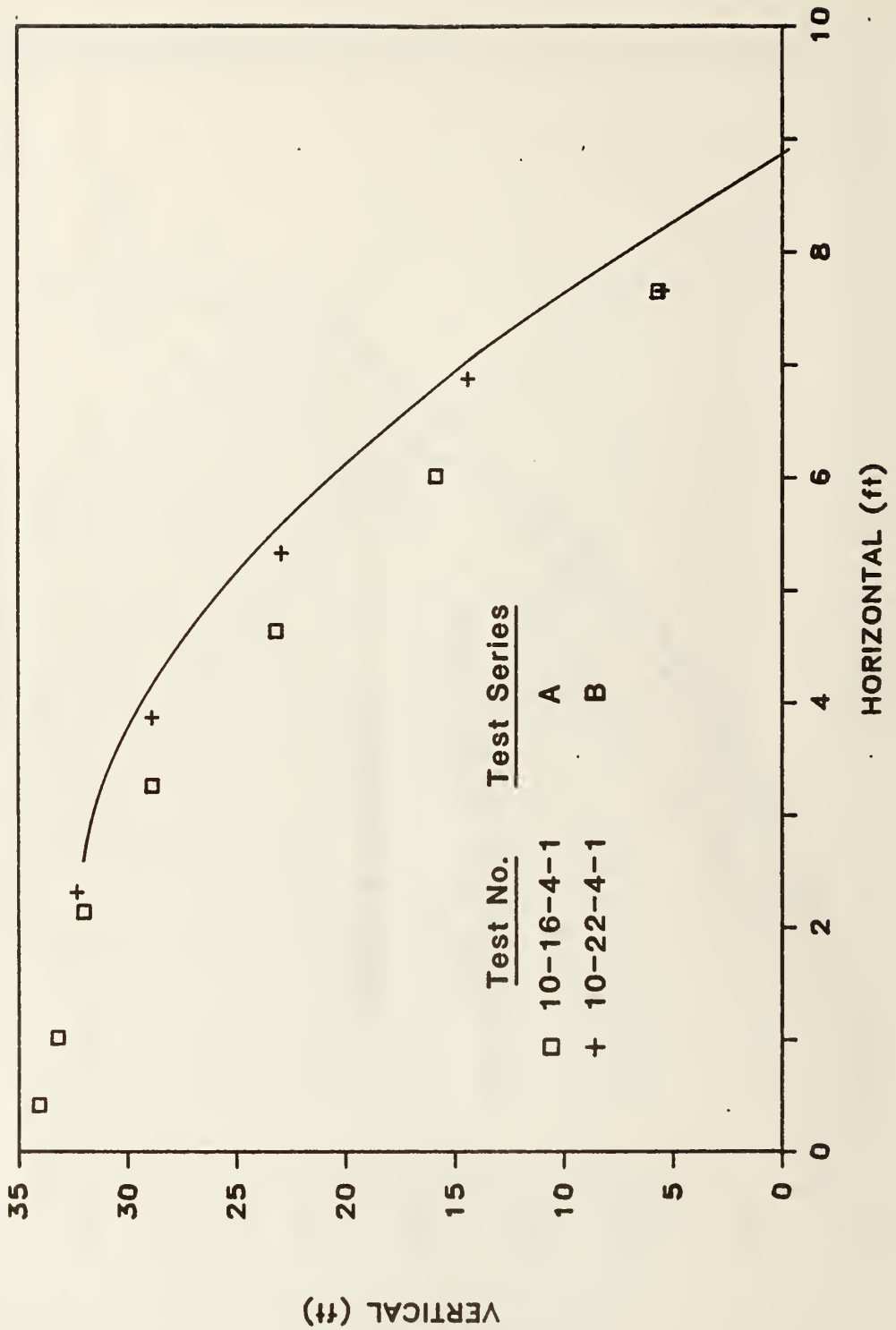

Figure 4.12 Measured locations of center of gravity for series A and B compared with computed trajectory

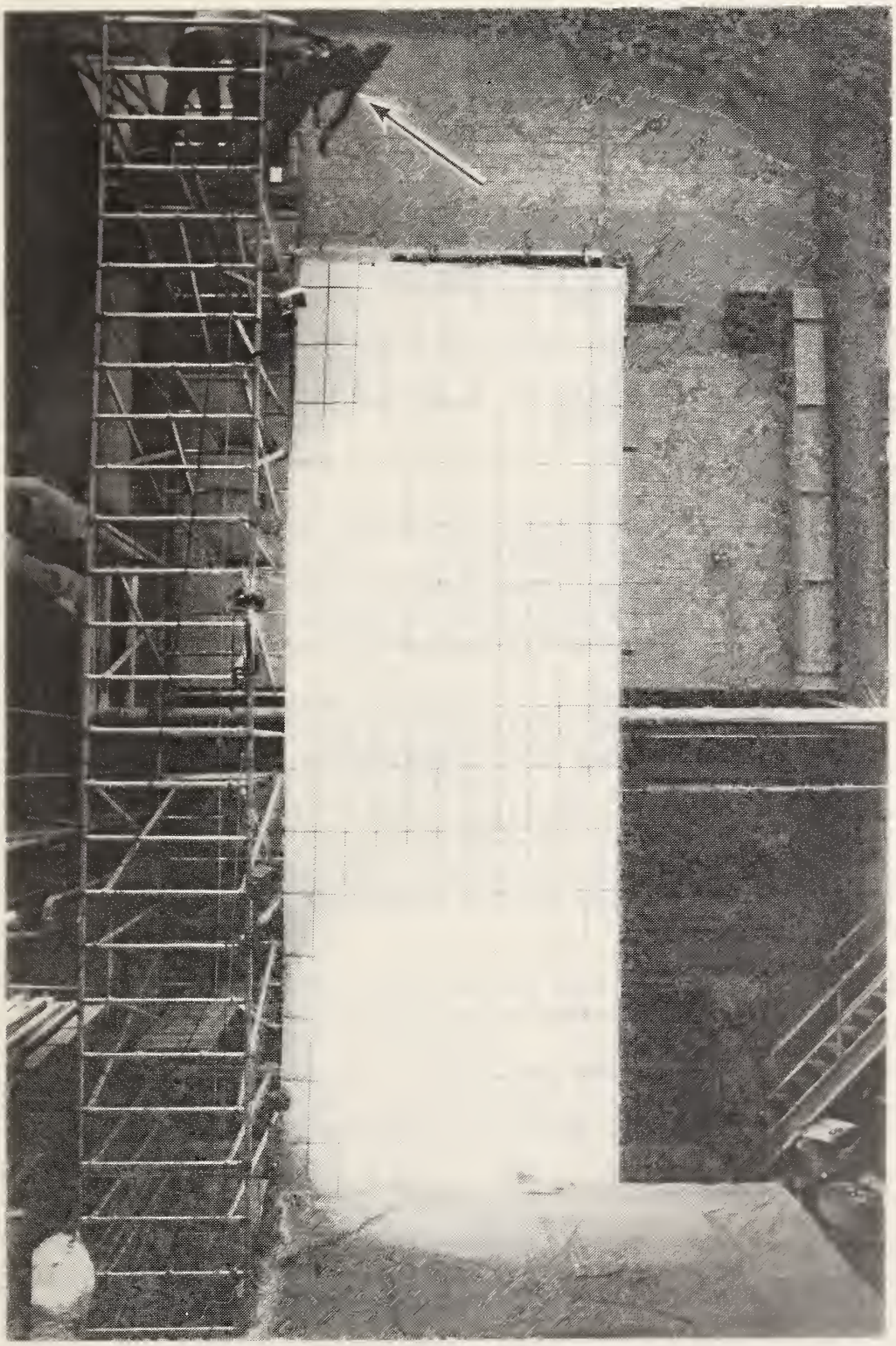

Figure 4.13 Position of dummy during test 11-7-4-1

position. As a result the center of gravity was closer to its feet than if the dummy were in the erect position. According to the parametric study, it is expected that a lower center of gravity would reduce the horizontal distance of the fall trajectory.

Figure 4.14 shows the measured trajectories for series C and D. It is seen that the data are consistent and the horizontal distances are significantly lower than for the forward facing test. The analytical model was used to compute the fall trajectory assuming a "lift-off" condition and assuming a height of the center of gravity of 2.5 feet (0.8 m). The computed trajectory is shown in figure 4.14. There is a good fit of the computed trajectory with the data points.

4.2.6 Summary

An analytical model was developed to predict the fall trajectories assuming the laboratory test conditions. The model assumes that the dummy behaves as a slender rod. While this might appear to be a crude approximation, comparisons of predicted trajectories with measured values showed that the predictions are generally satisfactory.

The analytical model was used to study the effects of the following parameters affecting the free-fall trajectories:

a) initial horizontal velocity;
b) height of the center of gravity;
c) coefficient of friction; and
d) "lift-off" as opposed to "sliding" at the start of free-fall.

The coefficient of friction had negligible effect on the trajectory. The initial horizontal velocity, as expected, did not have a strong effect on the trajectory. Decreasing the height of the center of gravity, reduced the horizontal distance. Likewise, changing from a "sliding" to "lift-off" as defining the start of free-fall causes a reduction in the horizontal distance.

5. DESIGN CONSIDERATIONS

The parametric study discussed in the previous chapter showed that for the fall conditions used in the testing program, the greatest horizontal fall distance occurs when the dummy, in an erect position, "slides" off of the platform. Physically this condition means that the center of gravity of the body is at its maximum distance from the feet, and that the pivot point of the body is at the edge of the platform. This fall condition results in the most conservative estimate of horizontal fall distances.

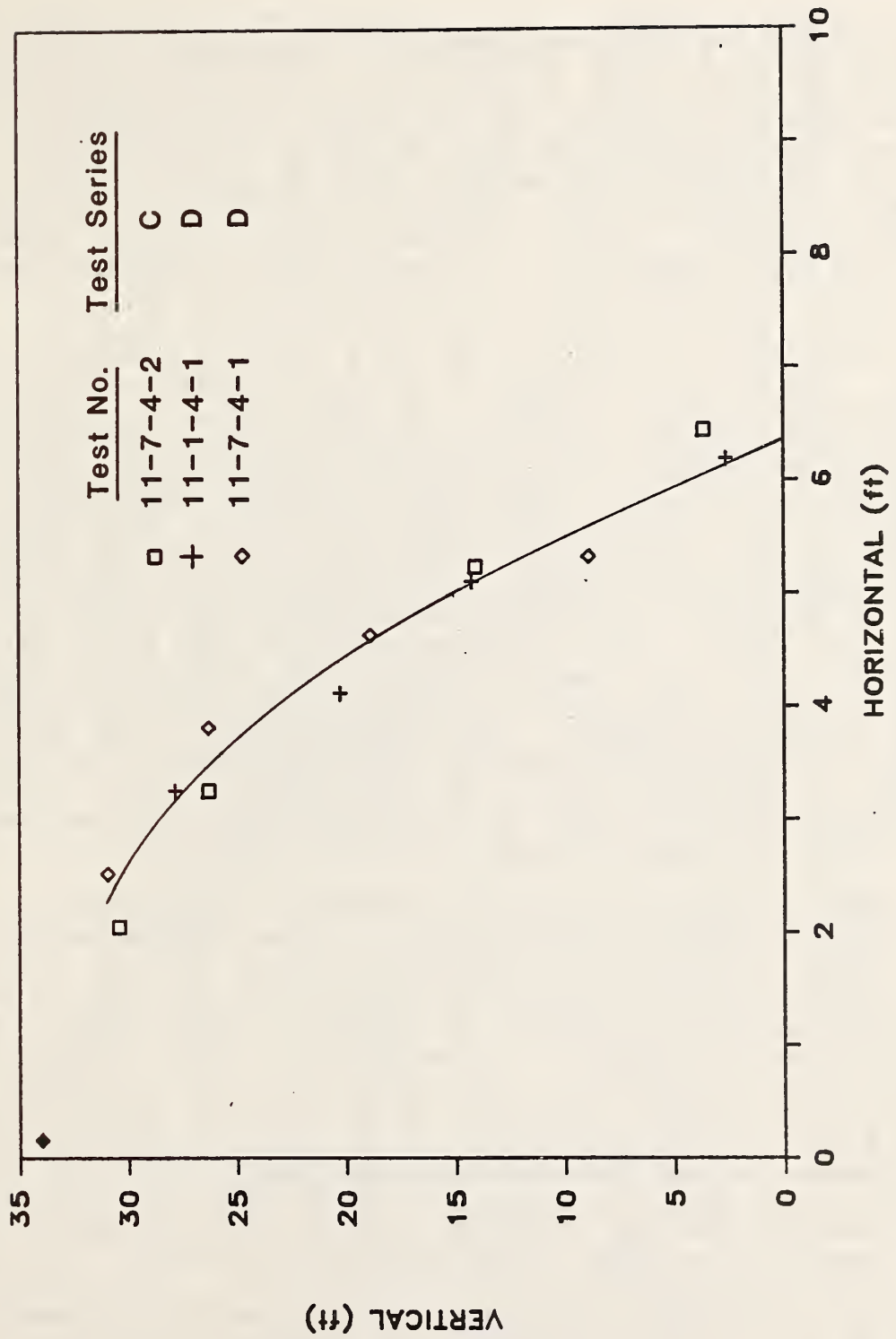

Figure 4.14 Measured locations of center of gravity for series C and D compared with computed trajectory

Figures 5.1 and 5.2 show the calculated trajectory of the center of gravity of the slender rod model as a function of the initial horizontal velocity. The vertical axis represents the distance below the working platform; the horizontal axis represents the horizontal distance from the edge of the working platform. Figure 5.1 was constructed using a value of 3.1 ft (0.95 m) for the center of gravity, which represents the value for an erect 50th percentile man. Figure 5.2 was constructed using a value of 3.4 ft (1.0 m)for the center of gravity which represents the corresponding value for an erect 95th percentile man.

These curves may be used to arrive at a rational answer to the question: "What should be the net projection distance so that a falling workman will be caught?" To answer this question, decisions must be made as to the size of the body that is to be caught and the maximum horizontal velocity with which this body will leave the working platform. In addition, the angular orientation of the falling body must be considered. Figure 5.3 shows two different angular positions of a body just before impact with the net. The dashed line represents the trajectory of the center of gravity of the body. In figure 5.3 (a) the body is nearly vertical at impact. The extreme part of the body (i.e. the head) will come to rest approximately a full body length away from the point indicated by the center of gravity. In figure 5.3 (b) the body is inclined at impact. The final position of the head in this case will be approximately half a body length away from where the center of gravity of the body hits the net. Thus, if the net is to catch the entire body, an additional distance must be added to the center of gravity distance obtained from figures 5.1 and 5.2.

As an example, suppose one wants to design a net projection to catch a body with proportions similar to the 95th percentile dummy. Using a conservative approach, assume the body falls with an initial horizontal velocity of 4 ft/s (1.2 m/s) (i.e., normal walking speed on the ground but a relatively fast speed on an elevated working surface). The net is to be hung 30 ft (9.1 m) below the working platform. From figure 5.2, the predicted location of the center of gravity of the body at impact is about 9 ft (2.7 m). If the body hits the net in an inclined position then an additional 3 ft (0.9 m) needs to be added to the 9-ft (2.7 m) distance if the net is to catch the entire body. If the body hits the net in a nearly vertical position, an additional 6 ft (1.8 m) needs to be added. This last case represents the worst condition - a required net projection of 15 ft. Taking a somewhat less conservative approach, using the 50th percentile dummy, falling 30 ft (9.1 m) with an initial horizontal velocity of 2 ft/s(0.6 m/s), figure 5.1 gives a predicted projection of the center of gravity of about 8.3 ft (2.5m). The height of the 50th percentile dummy is 5.7 ft(1.7 m). Thus,the required net projection to catch the entire body would be between 11.1 ft (3.4 m) and 14.0ft (4.3 m), depending on the inclination of the

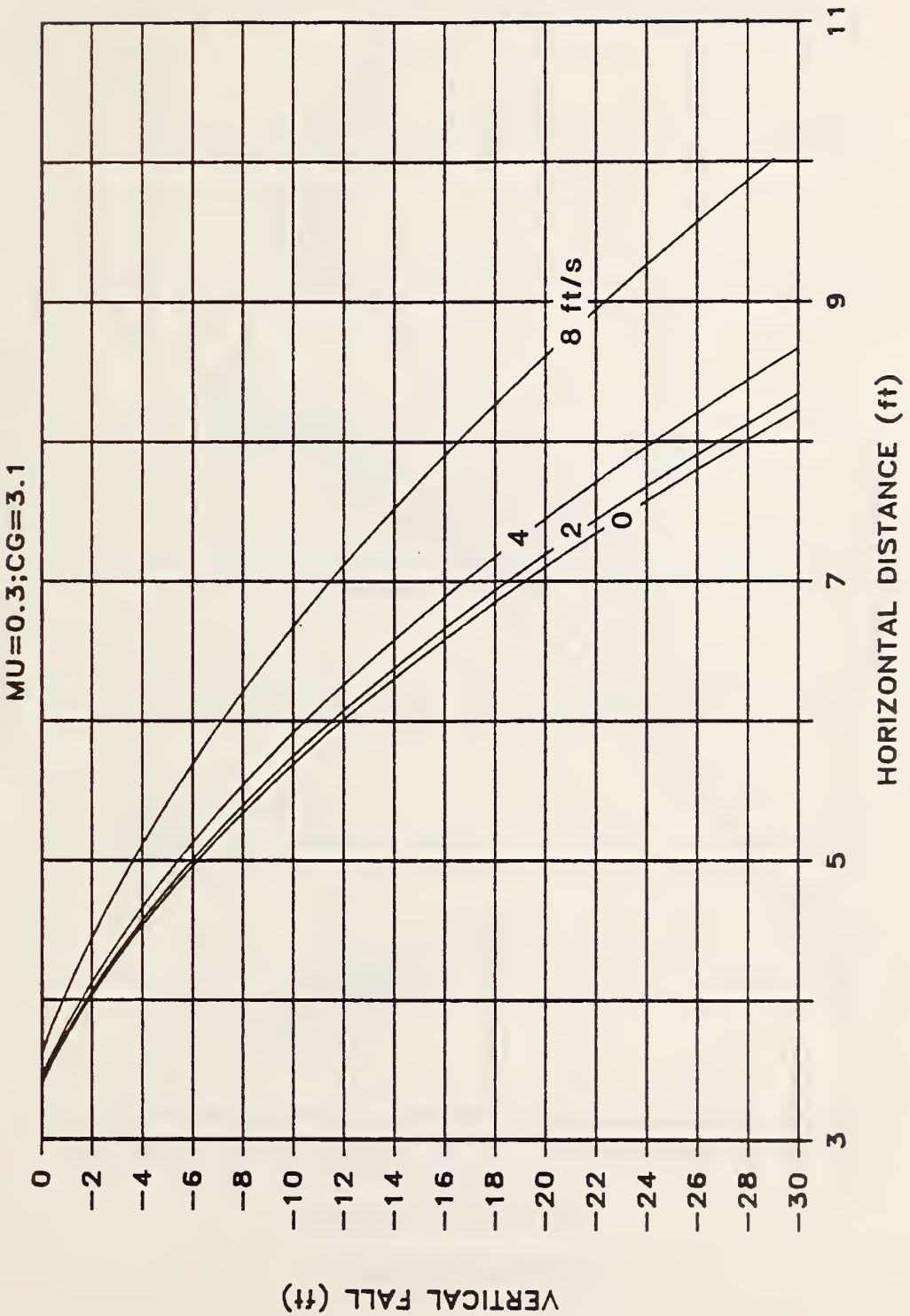

Figure 5.1 Location of center of gravity of 50th percentile dummy for various initial horizontal velocities

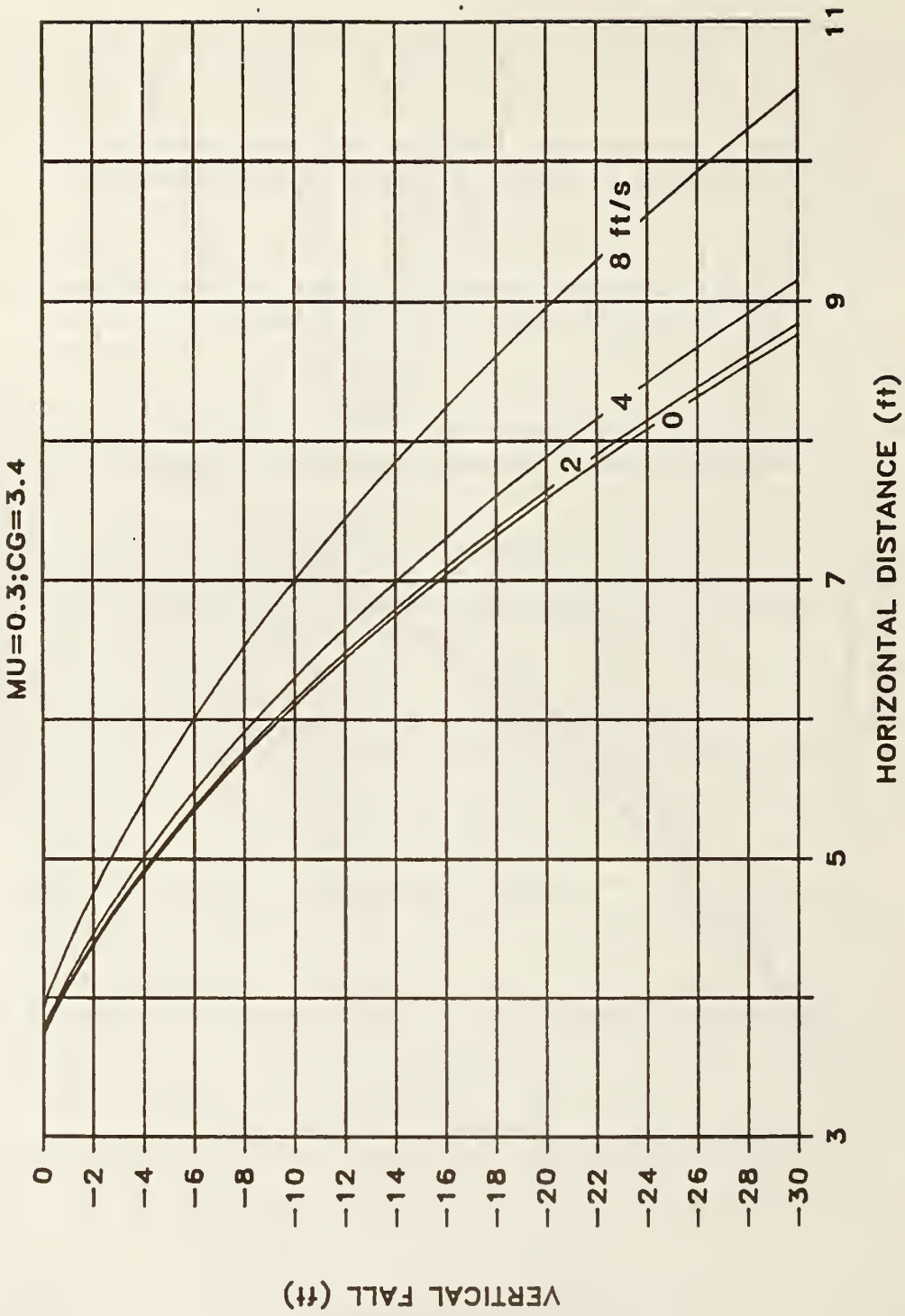

Figure 5.2 Location of center of gravity of 95th percentile dummy for various initial horizontal velocities

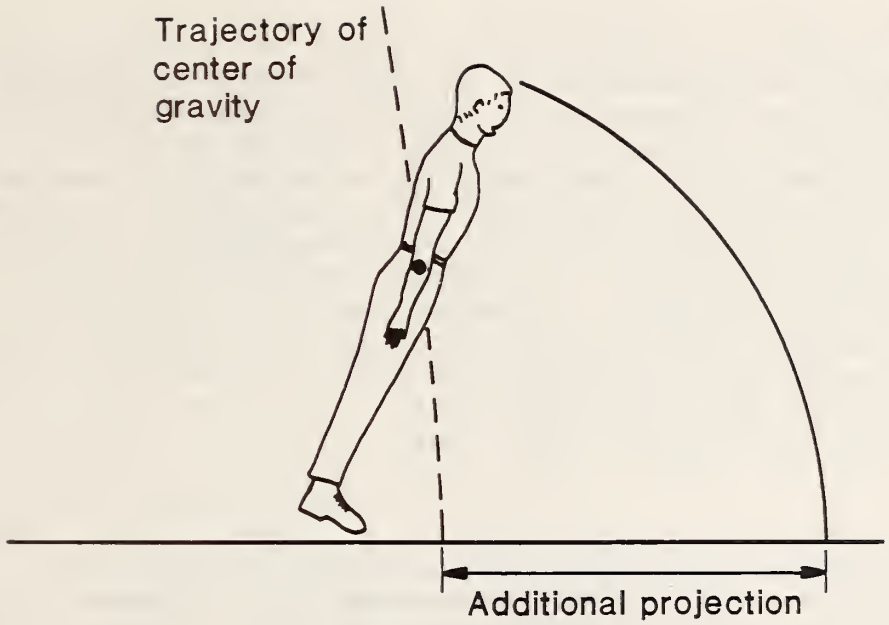

Figure 5.3a

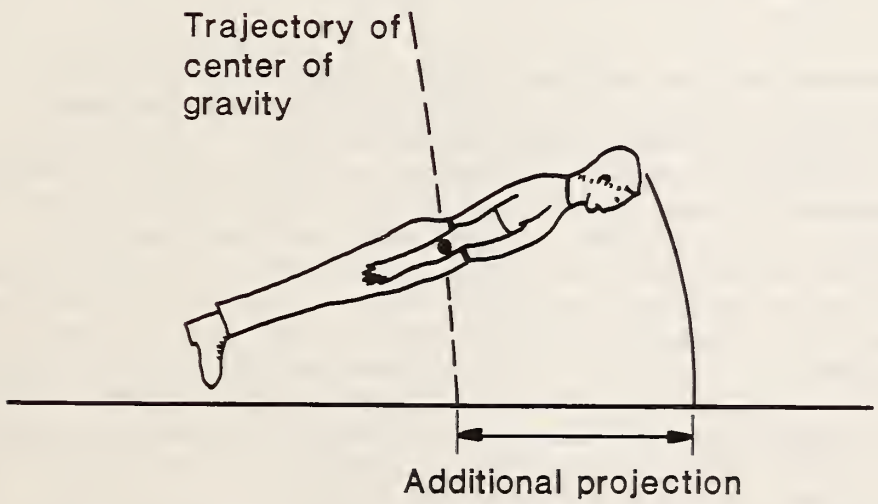

Figure 5.3b

Figure 5.3 Effect of angular orientation of body on landing position

body at the time it first hits the net.

Referring to the two examples above, if the maximum fall height is limited to 25ft (7.6 m) figures 5.1 and 5.2 indicate that the required net projection is reduced by about 0.5 ft (0.15 m). Thus, for the 95th percentile person with an initial horizontal velocity of 4 ft/s (1.2 m/s) the required net projection ranges between 11.5 ft (3.5 m) and 14.5 ft (4.4 m) depending on the body's angle of inclination at impact. Likewise, the 50th percentile person falling with an initial horizontal velocity of 2 ft/s (0.6 m/s) would require between 10.6 ft (3.2 m) and 13.5 ft (4.1 m) of net projection. In this manner, figures 5.1 and 5.2 can be used to establish design requirements.

6. SUMMARY

Of the several requirements applicable to perimeter safety nets, this study concentrated on the two dimensional requirements currently specified in OSHA Safety Standards: 1) minimum horizontal projection and 2) maximum fall height. The experimental program included 48 simulated fall tests with 50th and 95th percentile adult male dummies from a 30-foot-high platform. The investigative approach was to first identify the range of possible accidental fall events and to select for laboratory simulation the event that seemed most likely to cause the greatest horizontal displacement of a falling worker. The fall events selected involved walking, tripping, or stumbling over an obstacle which resulted in a worker falling from the edge of the working surface.

Based on the information in reference [2] regarding walking speeds and limited test data, it was concluded that "normal" walking speed is approximately 4.5 fps (2.0 m/s). Given that construction workers on elevated surfaces are not usually walking at even normal speed, it was felt that tests should be run with the dummies moving at a somewhat slower than normal walking speed. All of the tests were run with the dummies moving with a horizontal velocity of either 1.7 or 2.0 fps (0.5 or 0.6 m/s). The tripping event was simulated by stopping the trolley with a metal plate attached to the end of the track while permitting the continuance of the horizontal motion of the dummy's body. After undergoing rigid body rotation about the feet, the dummy either slid off or lifted off the trolley and underwent free fall until landing on the padded surface located 30 feet (9.1 m) below. The trajectory of the dummy's body was recorded photographically and its landing position was measured relative to the end of the trolley track. In addition to the slight variation in horizontal velocity and the difference in dummy sizes, the orientation of the dummy with respect to the edge of the platform was varied. Falls were conducted with the dummies facing forward, backward and sideways.

A long, slender rod model was developed to predict the trajectory of the body's center of gravity, given the fall event considered in the laboratory experiments. The analytical model was used to compute the angular velocity at the start of free fall, the horizontal and vertical positions of the center of gravity as it falls and the angular position of the rigid body. This model was used to conduct a study of the effects of varying several parameters: 1) initial horizontal velocity (i.e., walking speed), 2) length of the rod (i.e., worker's height), 3) weight of the rod (i.e., worker's weight), and 4) the coefficient of friction between the bottom of the feet and the working surface. In general, the analytical model gave good agreement with the experimental trajectory data. Where there was significant disagreement, the analytical model yielded slightly non-conservative trajectory predictions.

Considering all the experimental data (see table 3.1) without regard to the aforementioned variables, the calculated average landing distance for the 30-ft fall tests is 10.5 ft (3.2 m). Assuming that normal probability law statistics (i.e., a bell-shaped probability curve) can be applied to the fall test data, it would be expected that one-half of the landing distances exceed 10.5 ft (3.2 m) from the edge of the work platform. This distance to the extreme part of the body is significantly greater than the current minimum allowable perimeter net projection of 8 ft (2.4 m). In fact, when 3.1 ft (0.95 m) is subtracted from the average landing distance, the experimental results indicate a landing distance of 7.4 ft (2.3 m) for the center of gravity. Thus, for the fall event used in the laboratory tests, the location of the center of gravity, on average, was approximately 6 in (150 mm) from the edge of a hypothetical perimeter net that satisfies the current minimum requirements for horizontal projection. It is interesting to investigate the distribution of the test data above the sample average. The computed standard deviation for the entire set of test data is 1.2 ft (0.4 m). Applying the properties of a normal density function to the data, it is found that 75% of the horizontal landing distances would be less than 11.2 ft (3.4 m). In a like manner, 95% of the horizontal landing distances would be less than 12.4 ft (3.8 m). By subtracting 3.1 ft ((0.95 m) from the latter value, it is seen that the 95% limit for the center of gravity's landing distance is 9.3 ft (2.8 m).

The parametric studies show that the height of the center of gravity and whether free-fall occurs under a sliding or lift off condition are the two factors having the greatest influence on the trajectory. In the range of 0 to 4 fps (0 to 1.2 m/s) for the initial horizontal velocity, there is a narrow band of landing distances (see figures 5.1 and 5.2). Both the analytical and experimental results indicate that the fall trajectory is independent of weight.
It is emphasized that the experimental results and the companion

analytical model apply to the selected event of walking toward the edge, accidentally tripping over an obstacle, and falling from the edge of the work surface. It was felt that this represented a realistic set of worst-case conditions. It is recommended that these assumptions be critically evaluated by a panel representative of the construction community. To establish a consensus set of design requirements, the panel should recommend: a set of pre-fall conditions, a departure horizontal velocity, the statistical size of the worker (i.e., 50th or 95th percentile) and whether lift-off or sliding should be considered. Contingent upon the panel's recommendations, the analytical model may be refined and the envelope of predicted horizontal displacements modified to reflect the revised initial conditions. If the panel confirms the set of conditions that were simulated as a reasonable worst case, then there is a possibility of a worker's center of gravity projecting at least 7.5 ft (2.3 m) from the edge of the working surface when he falls 30 ft.

7. REFERENCES

1. Pielert, J. H., Status of Safety Net Standards for Construction and Research Needs, NBSIR 83-2709, National Bureau of Standards, Washington, D.C., September1983, 35 pp.

2. Levine, R. and Wolff, E., "Social Time: The Heartbeat of Culture," Psychology Today, Volume 19, Number 3, pp. 28-35, March 1985.

NBS-114A (REV. 2-8C)

U.S. DEPT. OF COMM. BIBLIOGRAPHIC DATA SHEET (See instructions)	1. PUBLICATION OR REPORT NO. NBSIR-85/3271	2. Performing Organ. Report No.	3. Publication Date

4. TITLE AND SUBTITLE

Perimeter Safety Net Projection Requirements

5. AUTHOR(S)

C. W. C. Yancey, N. Carino, and M. Sansalone

6. PERFORMING ORGANIZATION (If joint or other than NBS, see instructions)

NATIONAL BUREAU OF STANDARDS
DEPARTMENT OF COMMERCE
WASHINGTON, D.C. 20234

7. Contract/Grant No.

8. Type of Report & Period Covered

NBSIR

9. SPONSORING ORGANIZATION NAME AND COMPLETE ADDRESS (Street, City, State, ZIP)

Occupational Safety and Health Administration
200 Constitution Avenue, N.W.
Washington, D.C. 20210

10. SUPPLEMENTARY NOTES

☐ Document describes a computer program; SF-185, FIPS Software Summary, is attached.

11. ABSTRACT (A 200-word or less factual summary of most significant information. If document includes a significant bibliography or literature survey, mention it here)

Current construction-site safety net regulations set limitations on the minimum horizontal projection of perimeter nets and the maximum vertical distance between an elevated working surface and the net below. These limitations were arbitrarily established as no actual or simulated fall data existed. The adequacy of these requirements in ensuring construction worker safety has been questioned. Thus, a test program was carried out to determine the adequacy of existing regulations.

Simulated fall tests were conducted using anthropomorphic dummies to represent falling workers. The dummies fell from a 30-foot high platform and their trajectories were recorded photographically. The photographs were used to reconstruct the dummies' trajectories and to determine the horizontal distance between the face of the platform and the farthest point on a dummy's body. Results are presented to show the trajectory of the falling body and the maximum horizontal distance in the final landing position. An anlytical model was developed to simulate a falling worker. The model can be used to predict trajectories for a given set of initial conditions including worker height and weight, departure horizontal velocity and fall height. Guidelines are presented for revising existing regulations pertaining to the dimensional requirements for perimeter nets.

12. KEY WORDS (Six to twelve entries; alphabetical order; capitalize only proper names; and separate key words by semicolons)

construction safety; falling bodies; fall trajectory; horizontal distance; safety nets; simulated falls.

13. AVAILABILITY

☒ Unlimited

☐ For Official Distribution. Do Not Release to NTIS

☐ Order From Superintendent of Documents, U.S. Government Printing Office, Washington, D.C. 20402.

☒ Order From National Technical Information Service (NTIS), Springfield, VA. 22161

14. NO. OF PRINTED PAGES

15. Price